THERMODYNAMIC AND HYDRODYNAMIC PROPERTIES OF HYDROTHERMAL SYSTEMS

by

Henry J. Ramey, Jr.
William E. Brigham
H. K. Chen
Paul G. Atkinson
Norio Arihara

Stanford University
Stanford, California, U.S.A.

April 20, 1974

From the Proceedings of an NSF conference on "The Utilization of Volcano Energy," Hilo, Hawaii, February 4-8, 1974.

THERMODYNAMIC AND HYDRODYNAMIC PROPERTIES OF HYDROTHERMAL SYSTEMS

by

Henry J. Ramey, Jr., William E. Brigham, H. K. Chen,
Paul G. Atkinson, and Norio Arihara

Stanford University
Stanford, California

INTRODUCTION

Geothermal energy has received much attention in recent years as one of the sources that can help relieve the energy crisis in the next decade. There is considerable literature on the possible methods of geothermal energy extraction, and practical usage of geothermal energy is growing worldwide.

The goal of any geothermal production system is to extract heat from the earth, and to extract it at a high enough temperature and rate that it can be used commercially to generate power or process heat. Most present geothermal systems are geared toward power generation. To evaluate these systems we must predict the amount of heat present and the rate at which it can be extracted. These are the prime factors affecting the economics of any recovery process.

These two factors--amount of heat and recovery rate--in turn depend on basic physical properties of the reservoir rocks and the fluids contained within them. The amount of heat present depends on the heat capacity and density of the rock and the fluids within it. The rate of heat extraction depends on the thermal conductivity and the fluid flow characteristics, i.e., permeability and relative permeability, of the water and steam in the rocks. All these important basic characteristics of the rock and fluids are functions of both the temperature and pressure of the reservoir system.

Fortunately there is an extensive body of literature available to help one estimate many of these fluid and rock properties. Much of this information can be found in the petroleum literature, for the petroleum industry has had an interest in the use of underground heat for oil recovery since the early 1900's. In the paper we summarize some of the data that is useful for geothermal systems. A large fraction of these data are extracted from the petroleum literature.

STORAGE AND TRANSPORT OF HEAT IN ROCKS

Neglecting heat of phase change and heat of reaction, there are three important thermal properties in any process involving heat transfer: thermal conductivity, heat capacity, and thermal diffusivity. Thermal conductivity is generally shown by the symbol, k, and units in the c-g-s system are cal/sec-cm-°C. Many of the references, however, are given in British thermal units, Btu/hr-ft-°F. The conversion factor is:

$$1 \frac{\text{Btu}}{\text{hr-ft-°F}} = \frac{4{,}134 \times 10^{-3} \text{ cal}}{\text{sec-cm-°C}} \qquad (1)$$

The specific heat generally used is the specific heat at constant pressure, or $(\partial H/\partial T)_p$, and the symbol is C_p. The c-g-s unit, cal/gm-°C, is numerically the same as the British unit, Btu/lb-°F. Thermal diffusivity is a collection of terms, $k/\rho C_p$, where p is the density. It is often indicated by the symbol α. This grouping is the ratio of the ability to transfer heat, k, to the ability to store heat, ρC_p. In the c-g-s system the dimensions are cm^2/sec, and in the British system ft^2/hr. Many references use British units. The conversion factor is:

$$1 \frac{ft^2}{hr} = \frac{0.258\ cm^2}{sec} \qquad (2)$$

Thermal Conductivity

An early evaluation of rock thermal conductivity was made by Birch and Clark.[1,2] They studied a broad range of rock materials including some eighteen igneous rocks, seven sedimentary and metamorphic rocks, and certain single crystals and glasses. With the exception of the anorthosites and the glasses (both man-made and natural) all the materials showed a reduction of thermal conductivity with temperature increase. This behavior is as should be expected. See Figures 1 and 2, from Birch and Clark.[1]

Probably the most important finding by Birch and Clark was that the thermal conductivity of a mixture could be estimated by assuming that the various components of the system were in series. The total thermal resistivity of the system is equal to the volumetric weighted average of resistivity of each component. The total conductivity is thus the harmonic average:

$$\frac{1}{k_{ave}} = \frac{x_1}{k_1} + \frac{x_2}{k_2} + \ldots + \frac{x_n}{k_n} \qquad (3)$$

where x = volumetric fraction of each component.

Birch and Clark's data were mostly for rocks of low porosity. Somerton[3] was an early investigator of the thermal conductivity of fluid-containing rocks. He studied unconsolidated sands, sandstones, silty sandstones, siltstone, shale and limestone. He developed an empirical equation to predict the effect of fluid saturation on the thermal conducitivity of porous rocks. It was:

$$\frac{k}{k_1} = \left(\frac{k_2}{k_1}\right)^{c\phi} \qquad (4)$$

where k = thermal conduc ivity of flu i-saturated rock

k_1 = thermal conductivity of rock solids

k_2 = thermal conductivity of saturating fluid

ϕ = porosity - fraction

c = empirical constant approximately equal to 1.

The empirical constant, c, was actually found to range from 0.9 to 2.3 with the larger values found at Lower porosities. The product, $c\phi$, ranged from 0.325 to 0.460.

In 1961 Kunii and Smith[4] measured thermal conductivities of porous rocks saturated with various fluids. They proposed an equation (their Eqn. 3) to relate the fluid saturated conductivity to the conductivity of dry rock. Some of their results are reproduced here as Figures 3 and 4 to show the correspondence of their data to their model. Water may increase conductivity more than two-fold depending on the nature of the porous medium. Their data were run on Boise, Bartlesville, Berea and Rangely sandstones.

Smith and his coworkers[5,6] also studied the effect of fluid flow on the thermal conductivity of porous systems. In general they found that thermal conductivity in the direction of flow was increased as the flow velocity increased.' Figure 5 shows this effect with water and brine. They made a correlation of this effect through use of the product of the Reynolds' Number and the Prandtl Number (Fig. 6). Thermal conductivity perpendicular to the direction of flow, however, remained nearly constant--unaffected by flow rate.[6]

Anand, Somerton and Gomaa[7] recently have shown empirical methods of predicting thermal conductivities of fluid saturated rocks when there is little thermal data available. These methods are based on regression analysis equations. The thermal conductivity of dry rock (containing air) was correlated as follows:

$$\lambda_d = 0.3386\ \rho^{1.034} - 3.194\ \phi + 0.5304\ k^{0.100} + 0.0131\ F - 0.0311 \qquad (5)$$

where λ_d = thermal conductivity of dry rock, Btu/hr-ft-°F

ρ = bulk density, gm/cc

ϕ = fractional porosity

k = permeability, millidarcies

F = formation electrical resistivity factor

The formation resistivity factor is a common formation evaluation term which can be extracted from electric logs. It is the ratio of the actual resistivity to that if the rock pores were totally filled with formation water. In the absence of data on this parameter, the following empirical relationship can be used:

$$F = 1/\phi^m \qquad (6)$$

where m = cementation factor, often near 2.0 for sandstones.

Where the rock is fluid saturated the thermal conductivity is higher, and Anand, et al., found the following empirical equation was useful:

$$\frac{\lambda_s}{\lambda_d} = 1 + 0.299 \left[\left(\frac{\lambda_f}{\lambda_a} \right)^{0.330} - 1 \right]$$

$$+ 4.57 \left[\frac{\phi}{(1-\phi)} \frac{\lambda_f}{\lambda_d} \right]^{0.482m} \left(\frac{\rho_s}{\rho_d} \right)^{-4.30} \qquad (7)$$

where λ_s = thermal conductivity of fluid-saturated rock, Btu/hr-ft-°F

λ_f = thermal conductivity of the saturating fluid

λ_a = thermal conductivity of air

ρ_s = bulk density of saturated rock

ρ_d = bulk density of dry rock

Lastly, the effects of temperature were included. Anand, et al., used a modification of Tikhomirov's[8] correlation to show this effect. Their results were as follows:

$$\lambda_T = \lambda_{68°} - 0.709 \times 10^{-3} (T - 528) (\lambda_{68°} - 0.800) \cdot \left[\lambda_{68°} \left(T \times 10^{-3} \right)^{0.545\lambda_{68°} + 0.738} \right] \qquad (8)$$

where λ_T = thermal conductivity at temperature, T, Btu/hr-ft-°F

$\lambda_{68°}$ = thermal conductivity at 68°F

T = temperature, °R = °F + 460

A graph of their data compared to this equation is shown in Figure 7. The match appears to be satisfactory. The equation properly predicts that high conductivity materials have lower thermal conductivity at higher temperatures, while low conductivity materials exhibit increasing conductivities with temperature.

Often rocks contain *two* fluids rather than one. Gomaa and Somerton[9,10] discuss this effect in two recent papers. If both fluids are liquid, or if neither fluid is boiling or condensing, the thermal conductivity of the system is a simple square root relationship between the thermal conductivity and the fluid content, as follows:

$$\lambda - \lambda_1 = (\lambda_2 - \lambda_1)\ (S_2)^{1/2} \qquad (9)$$

where λ = thermal conductivity of rock containing two fluids

λ_1 = thermal conductivity of rock saturated with fluid 1

λ_2 = thermal conductivity of rock saturated with fluid 2

S_2 = the fraction of pore space filled with fluid 2

If the fluids are a liquid and vapor in equilibrium with each other, for example water and steam, the thermal conductivity may be far higher than predicted by Eqns. 8 and 9. The combination of heat transfer by boiling and mass flow by capillary pressure effects can cause the effective thermal conductivity to increase 2 to 5 fold. This is called the "heat pipe" effect. The amount of increase depends on the permeability of the rock, the latent heat of vaporization, the vapor saturation and the direction of heat flow with respect to gravity. The empirical equation they found to predict this additional term is as follows:

$$\lambda_{HP} = 0.003\ \phi^{0.357}\ k^{0.424}\ \frac{L\gamma}{\sqrt{\upsilon_\ell\ \upsilon_v}}\ (1 + 0.107\ \sin\phi)\ F(S) \qquad (10)$$

$$F(S) = \sin\left[\pi\left(\frac{1-S_\ell}{1-S_{\ell c}}\right)\right]\sin\left[\pi\left(\frac{1-S_v}{1-S_{vc}}\right)\right]$$

$$\cdot\left[0.74 + 0.61S_v + 1.56S_v^2 + 2.85S_v^3\right] \qquad (11)$$

$$S_{\ell c} = 0.098\ k^{-0.236} \qquad (12)$$

$$S_{vc} = 0.060\ k^{-0.236} \qquad (13)$$

where S_R and S_v = the fraction of pore space filled with liquid and vapor, respectively

ϕ = porosity, fraction

k = permeability, darcies

L = latent heat of vaporization, Btu/lb

γ = vapor pressure–temperature derivative, $lb/in^2-°F$

ν_ℓ and ν_g = viscosity of liquid and vapor, ft2/day

ψ = angle of heat flow direction, positive upward

λ_{HP} = additional thermal conductivity due to heat pipe effect, Btu/hr-ft-°F

By this stage, it should be clear that there is a problem in this study with respect to symbols and units. The symbol k has been used widely to represent both the thermal conductivity and permeability. Even the Greek symbol λ has been used often in various literatures to represent both heat and fluid conductivities of porous solids. Rather than totally recast equations in a single set of symbols and units, we have elected to preserve the symbols of the original study, where possible, and to define symbols and units where presented. This is done because the purpose of

of studies such as this is usually to guide a reader to further information, rather than to replace it. The pertinent literature is far too voluminous for a single paper to nerve a true summary purpose.

We turn now to a review of pertinent information on heat capacity and density.

Heat Capacity and Density

Somerton's[3] data on heat capacity of rocks shows that most reservoir materials behave similarly. Figure 8 shows some of the results of his work. Martin and Dew[11] point out that these data can be approximated roughly by a linear equation for heat capacity as a function of temperature:

$$c_p = \frac{T + 2000}{10{,}000} \qquad (14)$$

where c_p = heat capacity of rock, Btu/lb-°F

T = temperature, °F

Somerton also found that where rock is made up of minerals with many differing materials, the average heat capacity follows Kopp's Law, which states that the heat capacity is the mass weighted average of the constituents.

In general, rock volume changes only slightly with temperature. Further, many rocks containing large percentages of quartz behave much alike. Figure 9 shows the data of Somerton and Selim[12] for three sandstones and quartz. There is little difference in the results for the four materials.

Thermal Diffusivity

Because the thermal conductivity of many materials behaves similarly as a function of temperature, and because many materials have similar heat capacity–temperature behavior, it seems logical to expect that thermal diffusivity–temperature relationships will agree for many materials. The data of Somerton and Boozer[13] show that, indeed, many porous materials do exhibit similar trends in thermal diffusivity as a function of temperature. A notable exception was found with a tuffaceous sandstone, as seen in Figure 10; however, a fairly good approximating line could be drawn through the rest of the data in Figure 10. Thus use of this figure for quick estimation appears reasonable.

Heats of Phase Change and Reaction

In gas and oil reservoirs, very low heats of phase change and low heats of solution, plus the high heat capacity of the solid phase (rock) due to high mass of rock leads to nearly isothermal behavior for most fluid production thermodynamic paths. Exceptions are: (1) the process of oil recovery by underground combustion[57] and (2) oil recovery by steam injection.[58] The first involves release of large amounts of heat due to oxidation of a part of the oil, and the second releases heat by condensation of the injected steam. Actually several types of spontaneous oil oxidation reactions may occur leading even to ignition.[59] There appears little purpose to cite existing studies of oil oxidation reaction kinetics, other than to warn such information is available should pore space reactions become important in geothermal energy extraction. We turn now to a consideration of the effects of elevated temperatures on the flow characteristics of porous rocks.

TEMPERATURE AND PRESSURE EFFECT ON PERMEABILITY OF POROUS MEDIA

It is well known that the viscous flow of fluids through porous media follows Darcy's Law, which is expressed as:

$$v = -\frac{k}{\mu}\left[\frac{dp}{ds} - \rho g \frac{dz}{ds}\right] \tag{15}$$

where v is volume rate of flow across a unit area of the porous medium, k is permeability of the medium to a fluid at constant temperature, μ is viscosity of the fluid, p is pressure, ρ is the density of the fluid, g is the acceleration due to gravity, z is the vertical coordinate, and s is the coordinate along the direction of flow.

The permeability of a porous medium to a gas phase usually exceeds the permeability of the same medium to a liquid phase. The difference in these permeabilities is due to the phenomenon known as slip[14], reactions between liquids and the solid, and relative permeabilities. Slip is related to the mean free path of the gas molecules. Consequently, the permeability of a porous medium to gas should be a function of the temperature, pressure, and the nature of the gas. Klinkenberg[14] developed the relation between the permeability of a porous medium to gas and to a non-reactive liquid, viz:

$$k_g = k_\ell \left(1 + \frac{4c\bar{\lambda}}{r}\right) \tag{16}$$

This equation was derived assuming that all the capillaries in the porous medium are of the same diameter, and are oriented at random through the

solid material. In Eqn. 16, k_g and k_ℓ are permeabilities respectively to gas and to a single liquid phase completely filling the pores of the medium at constant temperature, $\bar{\lambda}$ is the mean free path of the gas molecules, r is the radius of capillaries, and c is a proportionality constant. Then, the mean free path can be expressed as:

$$\bar{\lambda} = \frac{1}{\sqrt{2\pi}\, d^2 n} = \frac{RT}{\sqrt{2\pi}\, p_m N d^2} \qquad (17)$$

where d is collision diameter, n is concentration of molecules per unit volume, N is Avogadro's Number, p_m is mean pressure, T is temperature, and R is universal gas constant.. Therefore, by combining Eqns. 16 and 17, we obtain:

$$k_g = k_\ell \left(1 + \frac{4CRT}{\sqrt{2\pi}\, rNd^2 p_m}\right) = k_\ell \left(1 + \frac{b}{p_m}\right) \qquad (18)$$

where b is called the Klinkenberg factor, which is constant for a given gas and a given porous medium at a constant temperature. As easily seen from Eqn. 18, a graph of k_g vs. $1/p_m$ should result in a straight line with an intercept of k_ℓ and a slope of bk_a as shown in Figure 11. Slope must become steeper as the temperature increases. Thus, the permeability to a gas is greater at low pressures, and is at a minimum at a maximum pressure of flow.

The permeability defined in Eqn. 15 requires that the porous medium is saturated completely with one homogeneous, single-phase fluid. The permeability thus defined is called the absolute permeability. When the

medium contains more than one fluid, the conductance of the medium to one fluid phase is commonly called the effective permeability. It depends on the volume fraction of each phase present in the pore space (called the saturation), the wetting characteristics of the fluids, and even the saturation history of the fluids. This will be discussed more thoroughly below. Another term, the relative permeability, is also commonly used. It is defined as the ratio of the effective permeability to some base absolute permeability value.

Wettability and Capillary Pressure

When more than one fluid exists in a porous medium, the static and flow properties of the medium depend upon the microscopic distribution of these phases within the pores. This distribution is controlled by the wettability of the porous medium. The wettability is the degree of preference of the porous medium surface for the various fluid phases. In petroleum engineering, water and oil are often considered wetting and non-wetting phase respectively. In geothermal systems that have water and steam coexisting in the same pore spaces, water will be the wetting phase and steam will be the non-wetting phase. Thus the discuesion that follows concerning oil and water can in many respects be directly related to steam-water systems.

Wettability of an oil-water-solid system is schematically shown in Figure 12.[15] The terms γ_{os} and γ_{ws} are surface tension between oil and solid, and between water and solid, respectively. γ_{ow} is interfacial tension between oil and water. θ is called contact angle. Then, for the equilibrium state:

Contact angles of less than 90°, measured through the water phase, indicate preferentially water-wet conditions, whereas contact angles greater than 90° indicate preferentially oil-wet conditions. The distribution of either the wetting or non-wetting phase within the pore spates does not depend solely upon the saturation of that phase, but depends also upon the direction of the saturaticn change. The terms "drainage" and "imbibition" refer to flow resulting in a decrease and increase, respectively, in the wetting phase saturation.

Since the wettability and direction of saturation change influence the fluid distribution, these factors would be expected to affect similarly both the capillary pressure and relative permeability characteristics. The capillary pressure, p_c, in porous media is defined as the pressure difference existing across the interface separating two immiscible fluids at rest, one of which wets the surfaces of the rock in preference to the other. The water-oil capillary pressure is defined as the pressure in the oil phase minus the pressure in the water phase, or:

$$p_c = p_o - p_w \qquad (20)$$

For the gas-liquid case (or steam-water):

$$p_c = p_g - p_\ell \qquad (21)$$

Figure 13 shows the capillary pressure characteristics of a strongly water-wet rock. It is seen in Figure 13 that the pressure in the oil phase (non-wetting) must exceed that in the water phase (wetting) before oil will enter the initially water-saturated rock. This would also be seen in a steam-water system. This entrance pressure is referred to as the threshold pressure

or displacement pressure. The minimum saturation point in Figure 13 gives the irreducible water saturation.

It has long been recognized that the vapor pressure above the curved surface of a liquid is a function of the curvature of the liquid surface. The capillary pressure is also a function of the curvature of the liquid surface. Considering that the liquid and vapor respectively are the wetting and non-wetting phases, the capillary pressure, pertaining to static equilibrium at curved surfaces of vapor-liquid phase separation, may be written as[16]:

$$p_c = p_g - p_{g'} + \frac{RT}{Mv_\ell} \ell n \frac{p_{g'}}{p_g} \qquad (22)$$

where p_g is the pressure in the vapor phase, $p_{g'}$ is the equilibrium vapor pressure of the liquid above a flat: surface, M is the molecular weight, and v_a is the specific volume of liquid. Then, the pressure in the liquid phase is:

$$p_\ell = p_{g'} - \frac{RT}{Mv_\ell} \ell n \frac{p_{g'}}{p_g} \qquad (23)$$

As the liquid is the wetting phase, p_g, is greater than $p_{g'}$. Then p_ℓ is smaller than $p_{g'}$. Therefore, if liquid pressures and temperatures are measured in the two-phase portion of the porous medium, liquid pressures must be lower than the normal (plane-surface) saturation pressures corresponding to the measured temperatures. Since capillary pressure values are a function of the liquid saturation, the vapor pressure lowering must be a function of the liquid saturation of the porous medium.

Relative Permeability

Figure 14 shows typical water–oil relative permeability characteristics for a water–wet core."' In this figure the permeability to oil at reservoir connate water saturation was used as the base value for relative permeabilities. These data were taken €or the case where the water saturation increased while the oil saturation decreased. If the data had been taken for decreasing water saturation, there would be a marked difference. The water (wetting phase) permeability data would be unchanged, but the oil (non–wetting phase) permeabilities would have been higher, especially at the right hand side of the graph. Further, the end points of the curves––the irreducible water saturation and the residual oil saturation––likely would have changed.

Muskat, et al.,[18] presented relative permeability curves for gases and liquids in unconsolidated sands, as given in Figure 15, which shows that for practical purposes the curves for the relative permeabilities k_{rg} and k_{rl} are independent of the nature of the unconsolidated sand. This is in marked contrast with most consolidated media, where the relative permeabilities must nearly always be measured, for they vary widely depending on the nature of the fluids and the porous system.

Temperature Effect on Relative Permeability

The relative permeability is affected by the test environment. The important factors are temperature, pressure, fluids and core condition. Several investigators have reported experimental results of the effect of temperature on relative permeability.

Poston, et al.,[19] using unconsolidated sand, found that the irreducible water saturation increased and the residual oil saturation decreased

with increasing temperature, as shown in Figures 16 and 17. This observation can be seen another way by considering Figure 14. In effect the higher temperature caused both relative permeability curves to shift to the left on the saturation axis. Poston, et al., speculated that if the relative permeability has changed, the capillary pressure should also be temperature sensitive.

Sinnokrot, et al.,[20] studied capillary pressure behavior of three consolidated sandstones and one limestone sample over a temperature range of 75° to 325°F by the restored state method. Their work confirmed the observation of Poston, et al., that the irreducible water saturation increased and apparent residual oil saturation decreased with increase in temperature. They concluded that capillary pressure curves for sandstones were displaced toward higher wetting phase saturations with an increase in temperature level, indicating an increase in water wetness with temperature level increase. Figure 18 shows part of their work.

Weinbrandt, et al.,[21] found results similar to Poston's when increasing from room temperature to 175°F in Boise sandstone. Representative data are shown in Figure 19. They also obtained data on absolute permeability in an increasing temperature level sequence from 75 to 315°F, as shown in Figure 20. The absolute permeability decreased drastically as temperature increased. Afinogenov[22] found similar results up to temperatures of 212°F.

Lo and Mungan[23] also studied relative permeabilities as a function of temperature and found results similar to Weinbrandt, et al. and Poston. They also studied systems of differing wetness characteristics and the results were found to be similar in both oil-wet and water-wet systems.

Poston, et al., pointed out that the changes in rock–fluid characteristics as functions of temperature level were all in a direction suggestive of an increase in water wetness with temperature increase. Contrary to this, Weinbrandt, et al., considered that temperature induced changes were too large to be explained by obvious factors such as change in contact angle interfacial tension, etc. They speculated that most of the above observations concerning temperature sensitivity may have been a result of thermally–induced mechanical stress. Work is continuing to attempt to clarify these results and the reasons for them.

Pressure Effect on Pore Volume

Von Gonten and Choudhary[24] investigated experimentally the temperature effect on pore volume compressibility, which is defined as:

$$c_f = -\frac{1}{V_p}\left[\frac{\partial V_p}{\partial p}\right]_T \qquad (24)$$

where V_p is pore volume and p is compacting pressure which is equal to overburden pressure minus pore pressure. Figure 21 is a plot of cumulative fractional pore volume change versus compacting pressure for sandstone at 75°F and 400°F. The pore volume compressibility, which is the slope of these curves, becomes smaller at higher pressure.

Somerton and Selim[12] showed the effect of temperature on sandstone volume, as indicated earlier in the paper in Figure 9.

Pressure Effect on Permeability

Afinogenov[22] presented data on the absolute permeability decrease as affected by external pressure. From his data he introduced an empirical formula to predict this effect:

$$\frac{k_p}{k_o} = \left(1 + \frac{127 \times 10^{-5}}{P}\right)^{-1} \qquad (25)$$

where effective pressure, p, is defined as:

$$P = p_{con} - 0.85\, p_{pore}$$

p_{con} and p_{pore} are confining pressure! and pore pressure respectively in atmospheres. He deduced that this permeability decrease was due to a decrease in the cross-sectional area of the pores and to a more torturous pore space configuration under the effect of pressure.

Zoback and Byerlee[25] measured the permeability of Berea sandstone as a function of both confining pressure and pore pressure. They reported that the permeability decreased with increased confining pressure, and increased as pore pressure was increased. Qualitatively, this agrees with Afinogenov's results. They found also that pore pressure had a significantly larger effect upon permeability than did confining pressure. This does e agree with the results of Afinogenov. They speculated that the matrix through which the fluid flows has a higher compressibility than does the granular framework through which the confining pressure stresses are transmitted.

Many other investigators, such as Fatt and Davis[26], Wyble[27], Dobrynin[28], Gray, et al.[29], and Wilhelmi and Somerton[30], have reported the effect of overburden pressure on the permeability of sandstone. Figure 22 is the

experimental results provided by Fatt and Davis. The permeability of sandstone decreased with increase in overburden pressure. Most of the decrease took place over the range of zero to 3000 psi overburden pressure.

PHYSICAL STATES OF WATER

The physical states of water of interest in geothermal reservoirs are: compressed liquid, saturated liquid, superheated (also called dry or unsaturated) steam, saturated (or wet) steam, and the dense fluid state.

The term "saturation" may thus have several meanings in geothermal reservoir engineering. "Saturation" can refer to: (1) the volume fraction of pore space occupied by a fluid phase, (2) the thermodynamic state of the fluid phases with reference to some appropriate vapor pressure curve, and (3) the usual sense of solids and gases being dissolved in a liquid phase. Care must be used that the term "saturation" is not misunderstood.

Figure 23 is a graph of the vapor pressure curve of water, showing the position of the critical point at 221.07 bar and 374.1°C (3206.2 psia and 705.4°F). Point A on this figure is in the superheated steam region, point B is at saturation conditions where both liquid and vapor may coexist, and point C is in the compressed liquid region. Points D and E are in the dense fluid region. Figure 24 is an expanded form of Figure 23 showing the initial thermodynamic state of various geothermal fields around the world. Note that the geopressured aquifers found in the Gulf Coast area of the United States, with temperatures of 260°C (500°F) and pres-

sures in excess of 700 bar (10,000 psia), are off the scales of both Figures 23 and 24, and might be considered as dense fluids.

Gibb's Phase Rule teaches that in order to specify the thermodynamic state of a single phase of water, two independent thermodynamic properties (e.g., pressure and temperature) must be specified. But if two phases are present (e.g., saturated steam and water) specification of only one intensive property defines the system. A geothermal aquifer at saturated conditions must follow some appropriate vapor pressure curve as fluid is produced.

It can be shown from thermodynamic analysis that a geothermal system initially containing a single-phase fluid (either compressed liquid or superheated steam) will tend to deplete isothermally. But once two phases form, a system should deplete along some sort of vapor pressure curve appropriate for the fluids in the pore space.

Properties of Interest

A thermodynamic equation of state for water expresses the pressure-volume-temperature (PVT) relationships. These describe the specific volume, v, (or density, $\rho = 1/v$) as a function of pressure and temperature for the various phases. In addition we require the energy related properties, specific enthalpy, h, and specific entropy, s,, and specific heats, c_p and c_v.

The transport properties that: are important are viscosity and thermal conductivity. Viscosity is basically an internal resistance of the fluid to flow, due to molecular interaction. Thermal conductivity affects the rate of heat transfer of the rock-fluid system.

Data describing the forementioned properties for impure water is meager, although a fair amount is known about the solubility of numerous substances found in geothermal waters. Ionic equilibrium calculations can be used to estimate which chemicals will remain dissolved, and which ones will precipitate under changing pressure, temperature, and composition conditions. The reader is referred to textbooks on geochemistry (Krauskopf[31]) and ionic equilibrium calculations (Butler[32]) and also to work on the chemistry of geothermal systems by White", Fournier and Truesdell[34], and Helgeson.[62]

Equations of State

Since the early part of this century there has been an international effort to standardize the various thermodynamic and transport properties of pure water. The well-known Keenan and Keyes[35] steam tables were a result of these efforts. The ASME Steam Tables[36] are one of the more recent products of these efforts, and are used as a basis for much of the data in this report. These tables present the results of a series of accurate matching of analytic! functions (the 1967 IFC Formulation for Industrial Use) to accepted and standardized experimental data (the 1963 International Skeleton Tables). The results are presented in tabular and graphical form. The analytic functions are also given, and can be pro-grammed for use on a computer. Another recent source of water .properties is the Steam Tables by Keenan, et al.[37]

The rest of this review will be devoted to describing the properties mentioned above, both for pure and impure water. Data will be presented in tabular or graphical form, and several simplified analytic forms will be discussed.

Pure Saturated Steam and Water

For conditions below the critical state (221.07 bar, 374.1°C; 3206.2 psia, 705.4°F) the liquid and vapor phases can coexist in equilibrium. When liquid and vapor are in equilibrium they are described as being saturated, and such states lie along the vapor pressure curve (see Figures 23 and 24). This curve is of great interest, and a number of simplified analytic approximations have been presented. A few will be given here. Whiting and Ramey[38] used an integrated form of the Clausius–Clapeyron equation to develop the following approximation by a least mean square curve match over the temperature range 150-315°C (300-600°F):

$$\ln p = \frac{-4667.0754}{(T + 273)} + 12.59833 \quad ; \text{ where } p = \text{bar}, \; T = °C. \qquad (26\text{–a}),$$

Or:

$$\ln p = \frac{-8400.7358}{(T + 460)} + 15.272703 \quad ; \text{ where } p = \text{psia}, \; T = °F. \qquad (26\text{–b})$$

This match is claimed to have an average difference from the actual data of only 0.048%.

In oil and gas technology, the Cox Chart is a useful empirical technique for representing the vapor pressure curves of hydrocarbon fluids. This is a graph of ln p vs. 1/(T-77.4), T in °R, and it is useful because both hydrocarbon and water vapor pressure curves tend to graph as straight lines. Thus, by choosing two points for water at opposite ends of the vapor pressure curve we can determine that the equation of this straight line is of the form:[61]

$$\ln p = \frac{-7001.4928}{(T + 382.2)} + 14.46928 \quad ; \text{where } p = \text{psia}, \; T = {}^\circ\text{F}. \qquad (27)$$

This function is a match over the whole vapor pressure curve, whereas the Whiting and Ramey approximation is for the range 150–315°C. Finally, Farouq Ali[39] observed that a graph of pressure vs. temperature on log-log paper yields a straight line. Hence:

$$T = 115.1\, p^{0.225} \quad (T = {}^\circ\text{F}, \; p = \text{psia}) \qquad (28\text{–a})$$

or

$$T = 116.7\, p^{0.225} - 17.778 \quad (T = {}^\circ\text{C}, \; p = \text{bar}) \qquad (28\text{–b})$$

Equation 28 is reported to have a maximum of 1% error over the pressure range 1–200 bar (10–3,000 psia).

The specific volume of saturated steam, v_g, and water, v_f, are shown as a function of pressure on Figure 25. The overall specific volume of mixtures of steam and water can be determined at a particular pressure (or temperature) if the quality, x, of the mixture is known. Quality is defined:

$$x \triangleq \frac{\text{Mass of mixture as steam}}{\text{Total mass of mixture}} \qquad (29)$$

The effect of quality on specific volume can be seen on Figure 25, and can be calculated from tables using the relation:

$$v_{mix} = x\, v_g + (1 - x)\, v_f$$

$$= v_f + x\, v_{fg} \quad , \qquad (30)$$

where v_{mix} = mixture specific volume

v_g = saturated gas specific volume

v_f = saturated liquid specific volume

$v_{fg} = v_g - v_f$

The second expression results in more accurate numerical results in hand calculations if steam quality is low.

The enthalpy of saturated steaim and water is shown as a function of pressure in Figure 26. Points B and C on this diagram correspond with those on Figure 23. There is a maximum enthalpy of 2.8 x 10^6 Joules/kg (1204.8 Btu/lb_m) that saturated steam may have under any conditions. This occurs between 31.16 and 31.85 bar (452 and 462 psia).

The overall enthalpy of saturated mixtures can be calculated from the relation:

$$h_{mix} = x\, h_g + (1 - x)\, h_f$$
$$= h_f + x\, h_{fg} \qquad (31)$$

where h_{mix} = mixture specific enthalpy

h_f = saturated liquid specific enthalpy

h_g = saturated gas specific enthalpy

h_{fg} = latent heat of vaporization per unit mass

The specific enthalpy of such mixtures is shown in Figure 26.

The latent heat of vaporization per unit mass, h_{fg}, is the increase in enthalpy as a fluid vaporizes from saturated liquid to saturated steam at constant pressure or temperature. At atmospheric pressure h_{fg} is approximately 2.3 x 10^6 Joules/kg (1000 Btu/lb_m). Farouq Ali[39] (p. 5) has presented the approximation:

$$h_{fg} = 1318\ p^{-0.08774} \qquad (32)$$

for use in hand calculations. The maximum error is reported to be 1.9%. The units used in Eqn. 32 are p, psia; h_{fg}, Btu/lb_m.

There appears to be some uncertainty about the viscosity of saturated steam and water. Accepted values are presented in the ASME Steam Tables. Figure 27 shows the viscosity of saturated steam and water vs. temperature. The viscosities of the two phases tend to approach one another as they approach the critical temperature.

Farouq Ali[39] recommends use of the following equation for the viscosity of steam:

$$\mu/100 = 88.02 + 0.32827\ T + 0.0002135\ T^3 - \rho\ (1858 - 5.90\ T) \qquad (33)$$

where μ = viscosity of steam, centipoise

T = temperature, °C

ρ = density of steam, gm/cc

The density of steam can be determined from steam tables. For pressures up to 1000 psia, the density of steam can also be determined from the following relation developed by Farouq Ali (p. 22):

$$\rho = 0.0000440189\ p^{0.9588} \qquad (34)$$

where ρ = density of steam, gm/cc

p = pressure, psia

The thermal conductivity of water first increases as the temperature increases and reaches a maximum at about 150°C. Thereafter it decreases. This is shown in Figure 28.

Impure Saturated Water

Chemical content will tend to have the same effect on the properties of saturated water and steam as they will on the unsaturated phases. Hence, with the exception of the vapor pressure curve, discussion of the effect of impurities will be postponed until later sections.

The vapor pressure of water in a geothermal system will not necessarily be that presented in the steam tables. For a fixed pressure, the boiling temperature of water will be elevated by the presence of impurities. This is equivalent to a lowering of vapor pressure. However, the effect is usually rather small. For example, at 4.621 bar (67.013 psia) pure water would boil at 148.89°C (300°F), whereas a 100,000 ppm (parts per million) sodium chloride brine would boil at 150.62°C (303.113°F). 'Chis difference would probably not be measurable in a geothermal system. However, significant vapor pressure lowering has been observed with production of 350,000 ppm brines in the Imperial Valley, California.

The vapor pressure data presented in steam tables were measured for flat surface interfaces. If the steam–water interface is a strongly curved surface, as might occur in small pores in porous media, then there could be significant vapor pressure lowering effects (Calhoun, et al.[40]; Edlefsen and Anderson[41]). Cady, Bilhartz, and Ramey[42] have investigated this phenomenon with regard to geothermal aquifers. They did not observe vapor pressure lowering in unconsolidated sandstone cores. However, a recent study by Strobel[56] indicates a potential vapor pressure lowering at very low liquid contents in experiments with a single, consolidated core. Continued experimentation is .in progress.

Pure Compressed Liquid Water

The compressed liquid region lies above the vapor pressure curves in the pressure-temperature planes of Figure 23 and Figure 24. Enthalpy and PVT behavior for compressed water is given in various tables[35,37] and in the ASME Steam Tables[36] for pressures up to 1070 bar (15,500 psia).

A technique commonly used in oil reservoir engineering for relating compressed water at some given reservoir condition to its state at surface conditions is via the formation volume factor, B_w. This is defined as the volume of liquid at reservoir conditions divided by the volume of liquid that would remain if it were brought to some standard surface conditions, commonly 20°C and 1 bar (70°F and 14.67 psia).

$$B_w \triangleq \frac{\text{initial volume of liquid at reservoir conditions}}{\text{volume of liquid remaining at standard conditions}} \qquad (35)$$

Figure 29 is a graph of the Formation Volume Factor, B_w, for pure liquid water as function of pressure and temperature. Note that for constant temperature, as pressure decreases, B_w increases slowly up to saturation conditions, below which it falls rapidly.

The specific volume-pressure behavior of a compressed liquid under an isothermal expansion or contraction process is often of interest (particularly in unsteady liquid flow through an aquifer). This P-V behavior is usually expressed in terms of the isothermal coefficient of compressibility, c_ℓ, which is defined:

$$c_\ell \triangleq -\frac{1}{v}\left(\frac{\partial v}{\partial p}\right)_T . \qquad (36)$$

c_ℓ can be viewed as the fractional decrease in specific volume caused by an isothermal unit increase in pressure. Although the isothermal compressibility of liquid water is often used in ground water hydrology and oil reservoir engineering, it appears to have been seldom reported for high values of temperature (greater than 120°C; 240°F). Table 1 summarizes high temperature results reported by Whiting and Ramey.[38] As can be seen, the isothermal compressibility for water is reasonably constant with pressure, but varies with temperature.

Table 2 presents the enthalpy of compressed pure water over a range of pressures and temperatures. It can be seen that the liquid enthalpy is only weakly dependent on pressure, but strongly dependent on temperature.

The viscosity of pure compressed water is presented in various Steam Tables.[35-37] The viscosity of high pressure liquid is almost constant with pressure, and generally only about 10–15% higher than the corresponding value for saturated liquid at the same temperature. Hence Figure 27, which shows the viscosity of saturated liquid as a function of temperature, can be used as a good estimate of compressed liquid viscosity.

The specific heat, c_p, of compressed water is also presented in the Steam Tables[35-37] for pressures up to 1035 bar (15000 psia). Values of c_p range from 4100 to 5000 Joules/Kg. °C (1.00 to 1.20 Btu/lb_m °F), except at temperatures greater than 260°C (500°F). Near the critical point values become very high.

Impure Compressed Water

The waters produced from geothermal systems often contain a dissolved chemical content high in chlorides and sulfates. Brines from some areas,

such as the Imperial Valley Salton Sea Geothermal Resource Area, have up to ten times the dissolved solids content of seawater. In addition, geothermal liquids often contain dissolved noncondensable gases.

Amyx, Bass and Whiting" (p. 450) state "Literature relative to the effect of composition on the properties (of water) is meager, and is limited to gas solubility data over the temperature range 32-250°F (0-121°C) at pressures ranging from 0–6000 psia (0-415 bar)." These authors summarize the work of numerous workers (Dodson and Standing[44], Rowe[45], Beal[46], Bridgman[47]) on the effect of natural gas solubility on the PVT behavior of water.

Long and Chierici[48] have presented experimental data on the PVT behavior of aqueous solution:; of sodium chloride. Their results were measured for temperatures over the range 20–100*o*C, pressures from 2-500 kg/cm^2, and salinities from 0-300g/L. They also presented analytic curve matches giving density,, p, as a function of salinity, pressure, and temperature over the range of experimental conditfons. It is unfortunate that data for higher temperatures were not measured. But results do give a quantitative indication of the effect of chemical composition on the PVT behavior of water.

Amyx, Bass and Whiting[43] (p. 466) present data from Van Wingen[49] on the viscosity of oil field brines at pressures to 7100 psia, and temperatures to 300°F. This data suggests that dissolved solids have only a small effect on the viscosity of saline brines. Stanley and Batten" have presented data on the viscosity of sea water compared to pure water from 0-30°C. They observed t'hat for practical purposes, the increase is not significant.

Although important information is available there is a need for PVT data for geothermal waters at conditions characteristic of geothermal reservoirs, showing the effect of chemical composition. In addition, more information is needed about the solubility and PVT characteristics of noncondensable gases dissolved in geothermal waters.

Pure Superheated Steam

Superheated steam occurs on the pressure-temperature plane at temperatures above the vapor pressure line, e.g., point A on Figure 23. This state is also called "dry" steam. The ASME Steam Tables[36] (1967, Table 3) present data for the enthalpy and PVT behavior of superheated steam for temperatures up to 815°C (1500°F). Figure 30 is a diagram showing the specific volume of dry steam as a function of pressure and temperature. One convenient means of calculating specific volumes of *dry* steam is via the real gas law equation of state:

$$Pv_g = \frac{zRT}{M} \qquad (37)$$

$$= z\bar{R}T$$

where P = pressure, bar

v_g = specific volume of steam, m^3/kg

z = gas law deviation (also compressibility) factor

$R = 0.08288 \ \frac{bar\ m^3}{kg_{mole}\ ^oK}$

M = molecular weight of water, $18\ kg/kg_{mole}$

$\bar{R}$ = RIM = $0.004605 \ \frac{bar\ m^3}{kg\ ^oK}$

T = absolute temperature, ^oK

OR, for English units

p = psia

v_g = ft /lb_m

$R = 10.72 \frac{\text{ft psia}}{16\ \text{mole}^\circ\text{R}}$

$M = 18\ lb_m/lb_{mole}$

$\bar{R} = 0.5956 \frac{\text{ft psia}}{lb_m\ ^\circ\text{R}}$

$T = {}^\circ\text{R}$

The gas law deviation factor, z, for steam is presented in Figure 31.

Figure 32 presents a pressure–enthalpy diagram for superheated steam. Point A on this diagram corresponds to point A in Figure 23. If a dry steam reservoir were to produce at constant temperature, its state would follow the isotherms on Figure 32. As indicated by the arrow below point A, the produced steam would tend to increase in enthalpy. Whiting and Ramey[••] have suggested that this tendency is a potential means of identifying the initial state of a geothermal fluid reservoir as dry steam.

Values for the viscosity of superheated steam are presented in the ASME Steam Tables[••] (1967, Table 10 and Fig. 7). Table 3 presents values of dry steam viscosity over a range of conditions. Except near the vapor pressure curve, the viscosity of dry steam is essentially independent of pressure, and is also only slightly higher than that of saturated steam at the same temperature.

The specific heat at constant pressure, c_p, of dry (and saturated) steam is presented in Table 9 of the ASME Steam Tables. Except near the vapor pressure curve and at higher pressures and temperatures, it is approximately 2100 J/kg-°C (0.5 Btu/lb_m-°F).

Mixtures of Dry Steam and Other Noncondensable Gases

Two of the recognized dry steam geothermal reservoirs in the world (the Geysers Field in California, and Larderello in Italy) are known to produce quantities of noncondensable gases along with their steam. Typically such gases contain carbon dioxide, hydrogen sulfide, ammonia, methane, and ethane. The quantity and proportions produced vary as a function of time, flow rate, and from well to well over the fields.

It is clear that the noncondensable gas content of a dry steam reservoir will effect the thermodynamic and transport properties of the produced fluid. Unfortunately, almost no experimental work seems to have been done on the properties of dry steam and noncondensable gas mixtures. However, generalized correlations have been extensively developed for natural gas mixtures of hydrocarbons. These correlations are based on reduced pressures and temperatures:

$$\text{Reduced Pressure, } p_r \triangleq \frac{\text{actual pressure}}{\text{pseudo critical pressure}} \tag{38}$$

$$\text{Reduced Temperature, } T_r \triangleq \frac{\text{actual temperature}}{\text{pseudo critical temperature}} \tag{39}$$

where the pseudo critical pressure and temperature are the molar average of the component critical values.

Amyx, Bass and Whiting[43] (pp. 260-268) have discussed and summarized correlations available for determining the PVT behavior of mixtures of natural gases with impurities such as nitrogen and carbon dioxide. On the basis of their discussion, the best method for estimating the effect of a noncondensable gas on steam compressibility appears to be through the use of an additive compressibility factor as first defined by Eilerts et al.[51]

$$Z_a = Z_{st} Y_{st} + Z_{ncg} Y_{ncg} \quad . \tag{40}$$

where Z_a = additive compressibility factor

Z_{st} = steam compressibility factor

Y_{ncg} = noncondensable gas compressibility factor

Z_{st} = Mole fraction steam in mixture

Y_{ncg} = mole fraction noncompressible gas in mixture

Amyx, Bass and Whiting[43] (pp. **260-268)** present graphs of the compressibility factor, **z,** for nitrogen (from Eilerts et al.[51]), carbon dioxide (from Olds et al.[52]), and hydrogen sulfide (from Reamer et al.[53]). For purposes of reservoir calculations, it is expected that the noncondensable gas content of many geothermal steams will have a minimal effect on PVT behavior.

The effect of noncondensable gases on geothermal steam viscosity is also of interest. Again, there appears to be almost no experimental data available, and we must resort to correlations. Amyx, Bass and **Whiting**[43] (pp. **278-286)** present the results of numerous correlations for natural gases. On the basis of their discussion, **a** rule proposed by Herning and **Zipperer**[54] for calculating the viscosity of mixtures of gases appears to be the most promising correlating method. In this rule the viscosity of the mixture, μ_m, is given by

$$\mu_m = \frac{\sum_{i=1}^{n} \mu_i Y_i M_i}{\sum_{i=1}^{n} Y_i M_i} \tag{41}$$

where μ_m = viscosity of mixture

μ_i = viscosity of i^{th} component

M_i = molecular weight of i^{th} compcnent

Y_i = mole fraction of the i^{th} component in mixture

n = total number of components in the mixture

Basically this is an averaging calculation weighted by the mass of each component present. The viscosity of various gases over a range of temperatures can be found in standard physical properties reference books (e.g., see Weast[55], pp. F41-F44). For practical purposes, the noncondensable gas content will not significantly affect the viscosity of most geothermal steams.

A Note on Units

In general, equations and numerical values have been expressed in metric units (bar, ^oC, m, kg), with values for engineering units given in parenthesis (psia, ^oF, ft, lb_m). Viscosity is given in centipoise. For convenience of writing this is not true in every case. Units are always specified where equations are presented throughout the paper.

Note the following conversions:

Pressure:	1 psia	=	0.06895 bar
	1 bar	=	1.0197 kg/cm^2
	1 bar	=	0.9869 atm.
Specific Volume:	1 ft^3/lb_m	=	0.062428 m^3/kg
	1 ft^3/lb_m	=	62.43 cc/gm
Enthalpy:	1 Btu/lb_m	=	2324.4 Joules/kg
Yiecosity	1 c.p.	=	6.72×10^{-4} lb_m ft sec
	1 c.p.	=	2.089×10^{-5} lb_F sec/ft^2

Acknowledgment

Preparation of this report was funded by the National Science Foundation as a portion of the study "Stimulation of Geothermal Aquifers," Grant No. GI-34925, principal investigators Drs. Paul Kruger and Henry J. Ramey, Jr., Stanford University.

TABLE 1

Isothermal Compressibility of Liquid Water, $psia^{-1}$

p,psia	300°F	400°F	500°F
700	3.793×10^{-6}	5.811×10^{-6}	7.146×10^{-6}
800	3.795×10^{-6}	5.815×10^{-6}	7.152×10^{-6}
1000	3.913×10^{-6}	5.821×10^{-6}	10.703×10^{-6}

TABLE 2

Enthalpy of Compressed Water in Btu/lb

and Joules/kg [(Btu/lb)/(J/kg)] at Various Pressures and Temperatures

(Data fr[illegible] Ref 3[illegible]

Temperature		Pre[illegible]ure, [illegible]i[illegible]/bar				
°F	°C	100/6.9	500/34.5	1000/69.0	2000/138.	5000/345
[illegible]0	21	38.33/8.91x10^4	[illegible]9 [illegible]/9 1[illegible]x10[illegible]	[illegible]0 82/9 [illegible]9x10[illegible]	[illegible]3 [illegible]/1.01[illegible]0^5	51.7/1.202x10^5
200	93	1[illegible]8.3/3.91x10^5	1[illegible]9.2/3 93x10^5	1[illegible]0 3/3 9[illegible]x10[illegible]	1[illegible]2.6/4.01x10[illegible]	1[illegible]9.5/4.17x10^5
[illegible]00	20[illegible]	X	375.4/8.[illegible]3x10^5	3[illegible].0/8 74x10^5	3[illegible].2/8 7[illegible]x10^5	381 2/8.8[illegible]x10[illegible]
[illegible]00	31[illegible]	X	X	X	[illegible]14.5/1 43x10[illegible]	[illegible]0[illegible].6/1[illegible]0x10[illegible]

TABLE 3

Viscosity in Centipoise of Superheated Steam at Various Conditions

(Data from Ref 36)

Temperature		Saturation Conditions			Pressure psia / bar						
°F	°C	P, psia	P, bar	,c.p.	1/.06895	5/.345	10/.690	50/3.45	100/6.9	500/34.5	1000/69
200	93	11.5	.79	.01	.012	.012	.012	X	X	X	X
300	149	67	4.62	.014	.014	.014	.014	.014			
400	204	247.3	17.1	.0155	.016	.016	.016	.016			
500	260	681	47.0	.0177	.0186	.0186	.0186	.0186	.0186	.0180	
600	316	1543	106.4	.02	.02	.02	.02	.02	.02	.02	.02

FIGURE 1

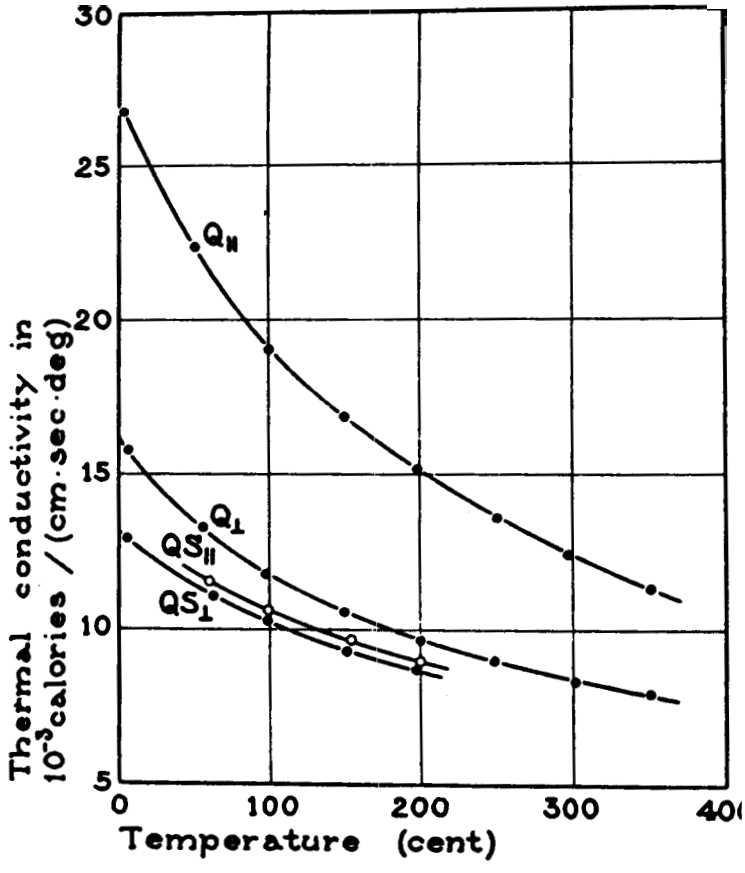

Thermal conductivity of quartz and of a quartzitic sandstone.

$QS_{\perp}$ Quartzitic sandstone, Penn., $\perp$ bed-plane.
$QS_{\parallel}$ Quartzitic sandstone, Penn., $\parallel$ bed-plane.
$Q_{\perp}$ Quartz single crystal $\perp$ optic axis.
$Q_{\parallel}$ Quartz single crystal $\parallel$ optic axis.

(Ref. 1)

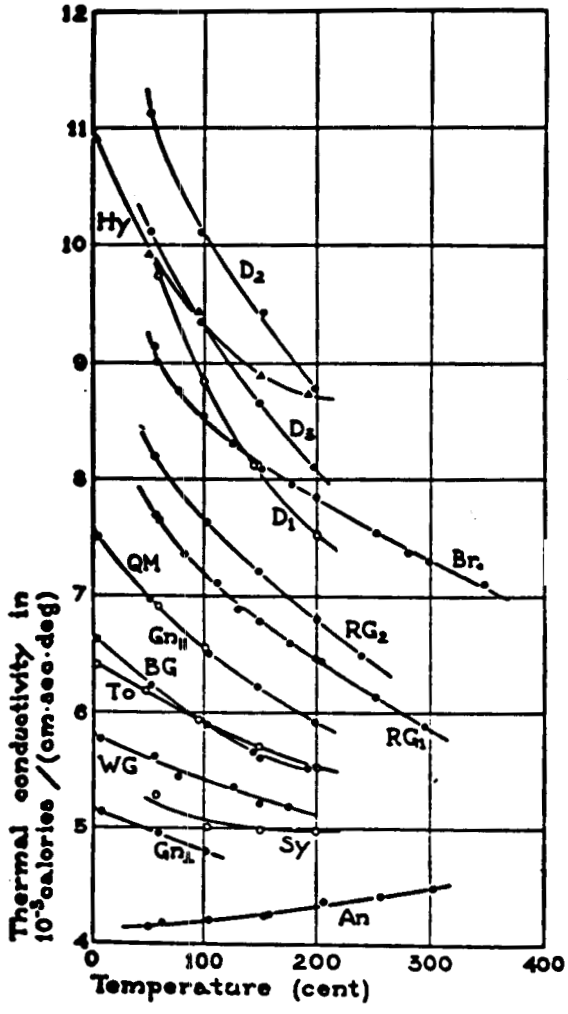

FIGURE 2 **Thermal** conductivity of holocrystalline rocks. (Ref. 1)

An	Anorthosite, Quebec.	RG,	Rockport Granite 1.
Gn⊥	**Gneiss,** Pelham, ⊥ bed-plane.	RG,	Rockport Granite 2.
Gn∥	Gneiss, Pelham, ∥ bed-plane	Br	Brontitite.
Sy	Syenite, Ontario.	Hy	Hypersthenite.
WG	Westerly Granite.	D_1	Dunite 1.
To	Tonalite, Calif.	4	Dunite 3.
BG	Barre Granite.	4	Dunite 2
QM	Quarts monzonite, Calif.		

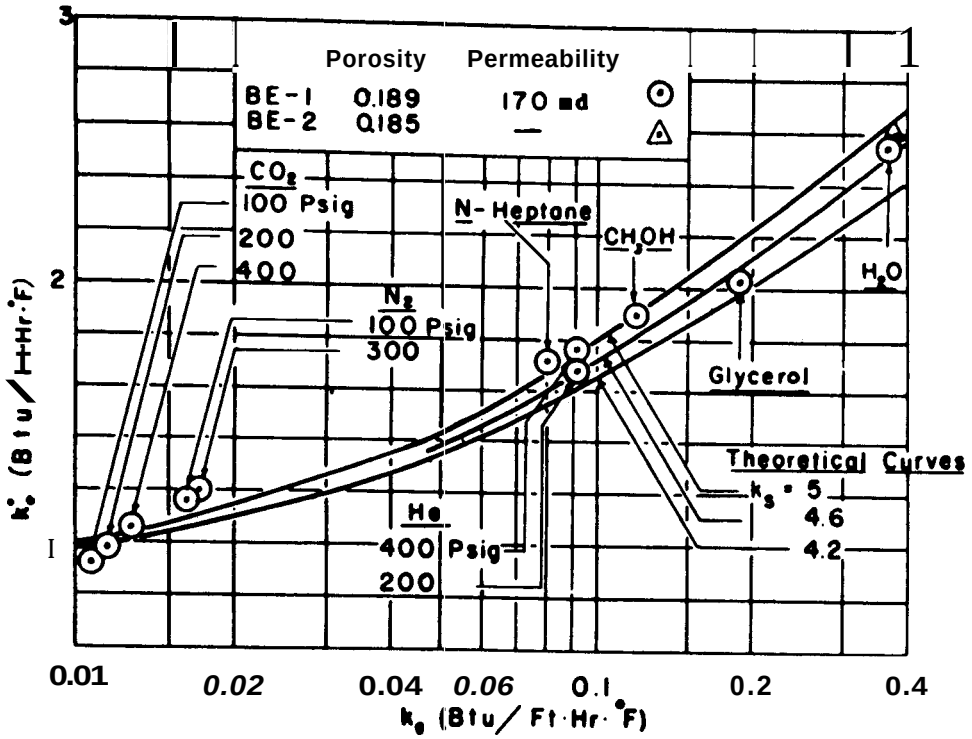

FIGURE 3 — **STAGNANT CONDUCTIVITIES VS CONDUCTIVITIES OF FLUIDS, BEREA SANDSTONE.** (Ref. 4)

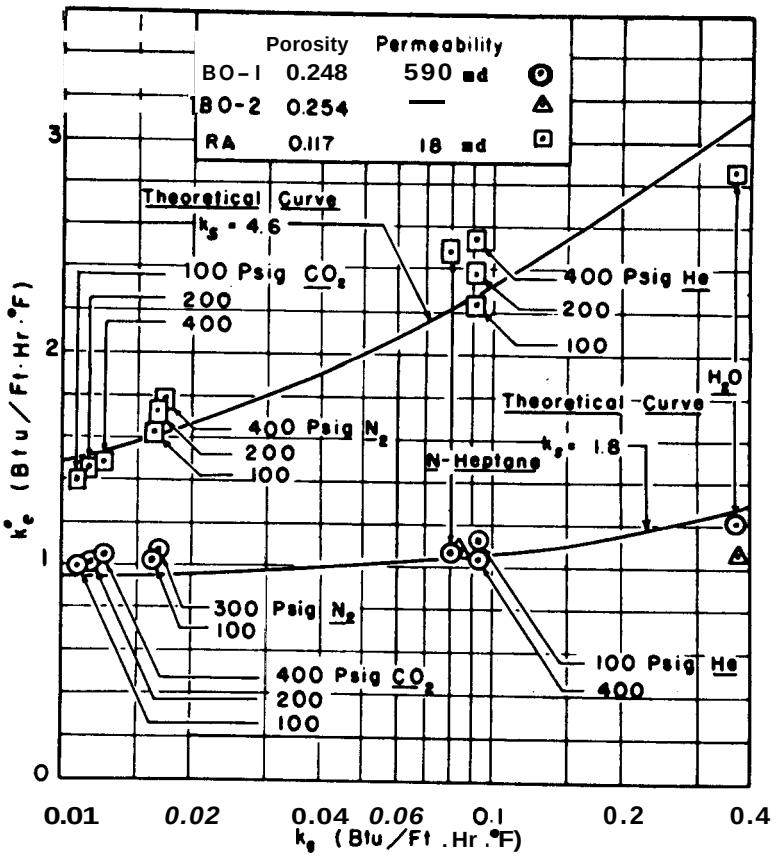

FIGURE 4 – STAGNANT CONDUCTIVITIES VS CONDUCTIVITIES OF FLUIDS, BOISE AND RANGELY SANDSTONES.

(Ref. 4)

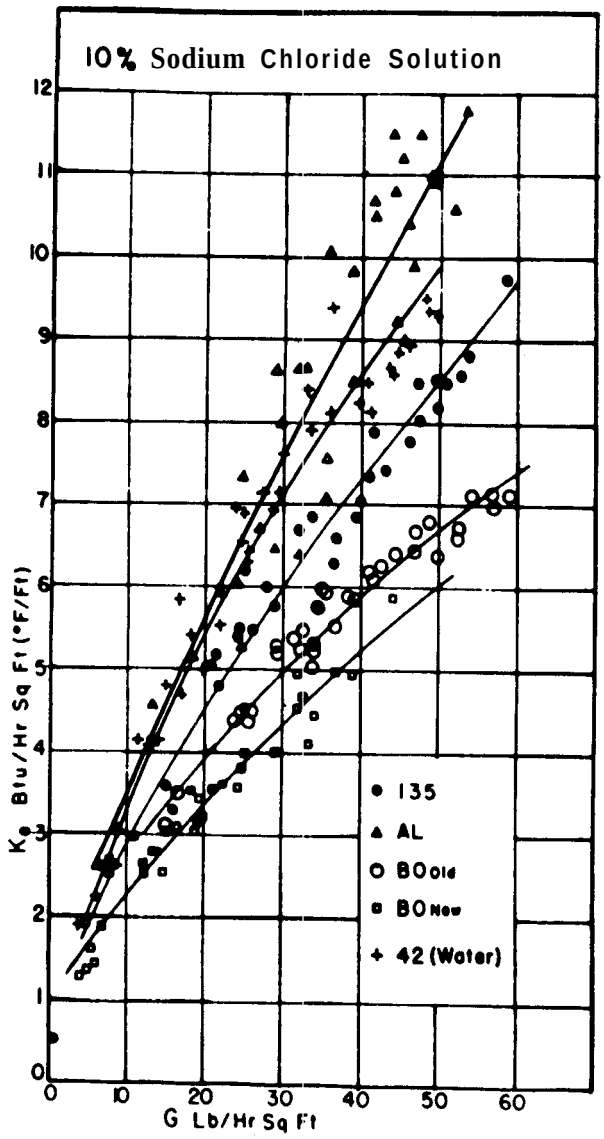

FIGURE 5 — Effective thermal conductivity (Ke) as a function of mass flow rate (G). See Ref. 5 for legend. (After Adivarahan, Kunii and Smith, Courtesy Soc. of Petrol. Engrs. of AIME.) (Ref. 5)

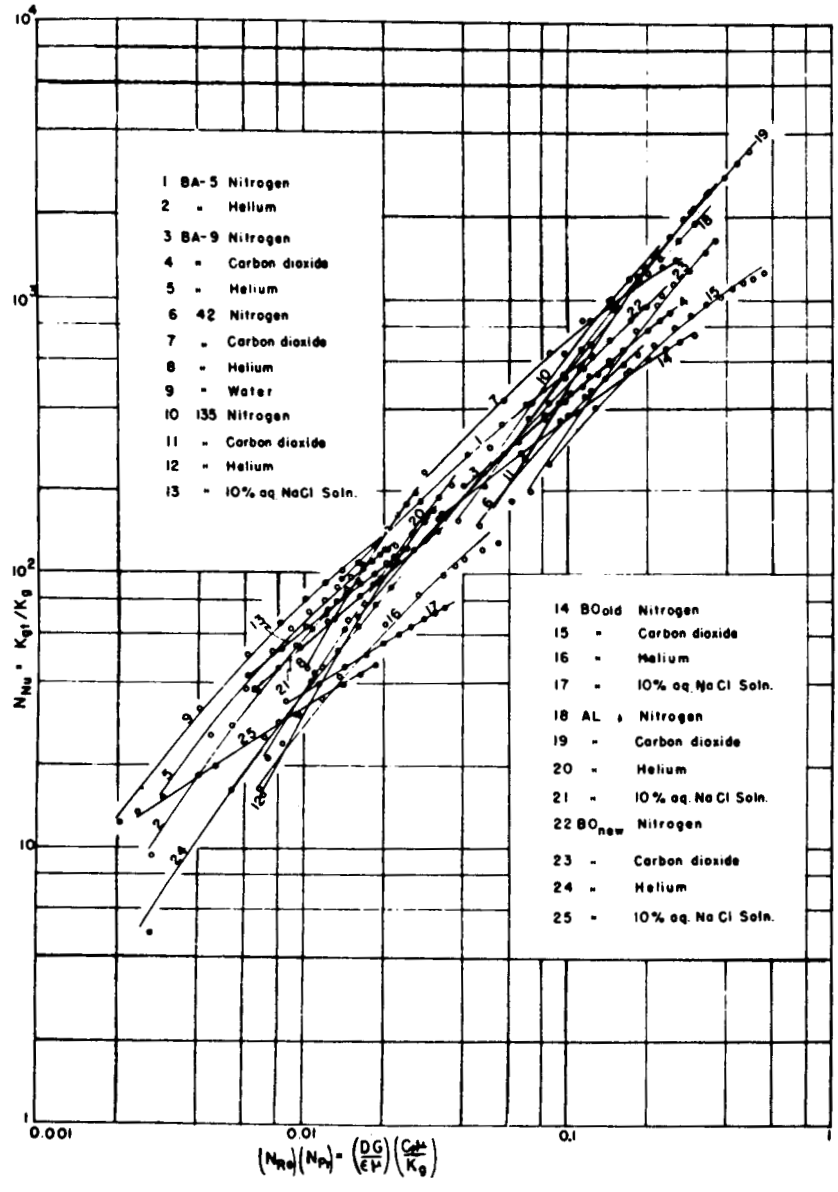

FIGURE 6 — CORRELATION OF k_{gt}/k_g WITH $(DG/\epsilon\mu)(C_p\mu/k_g)$. (Ref. 5)

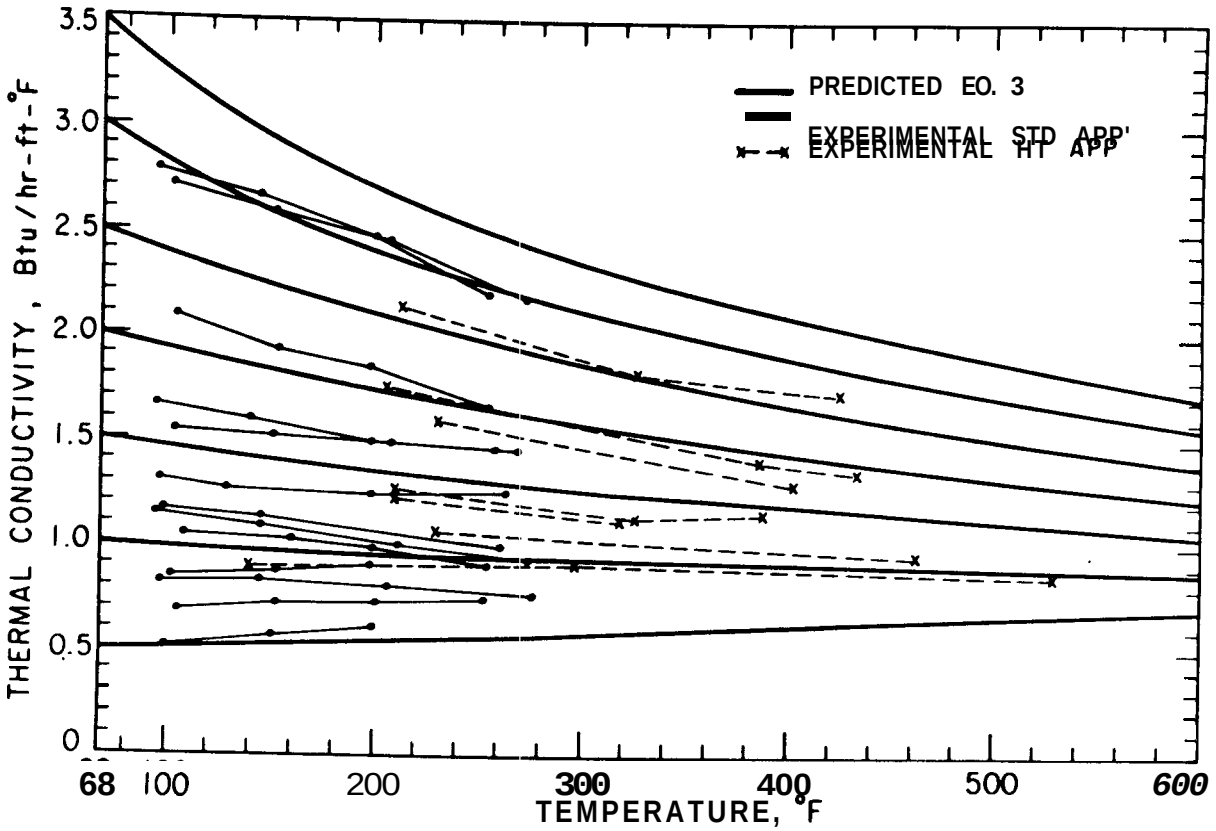

FIGURE 7 Effect of Temperature on Thermal Conductivity of Sandstone. (Ref. 7)

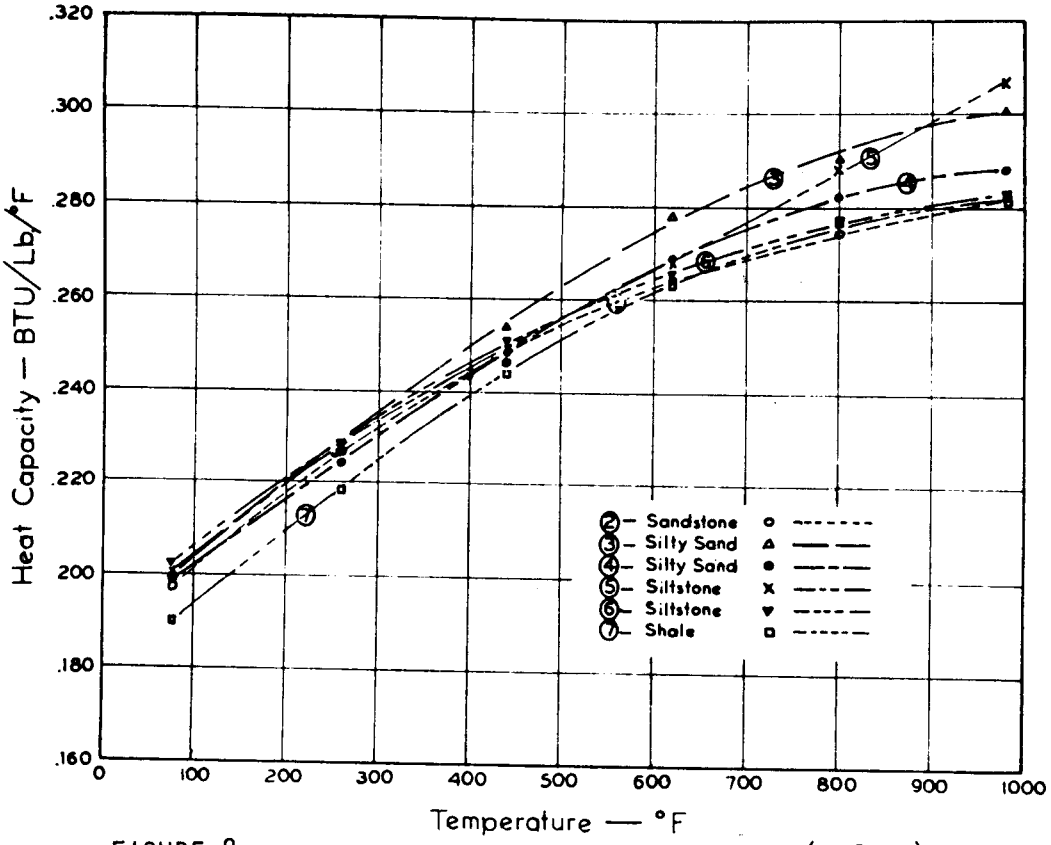

FIGURE 8 —EXPERIMENTAL HEAT CAPACITIES. (Ref. 3)

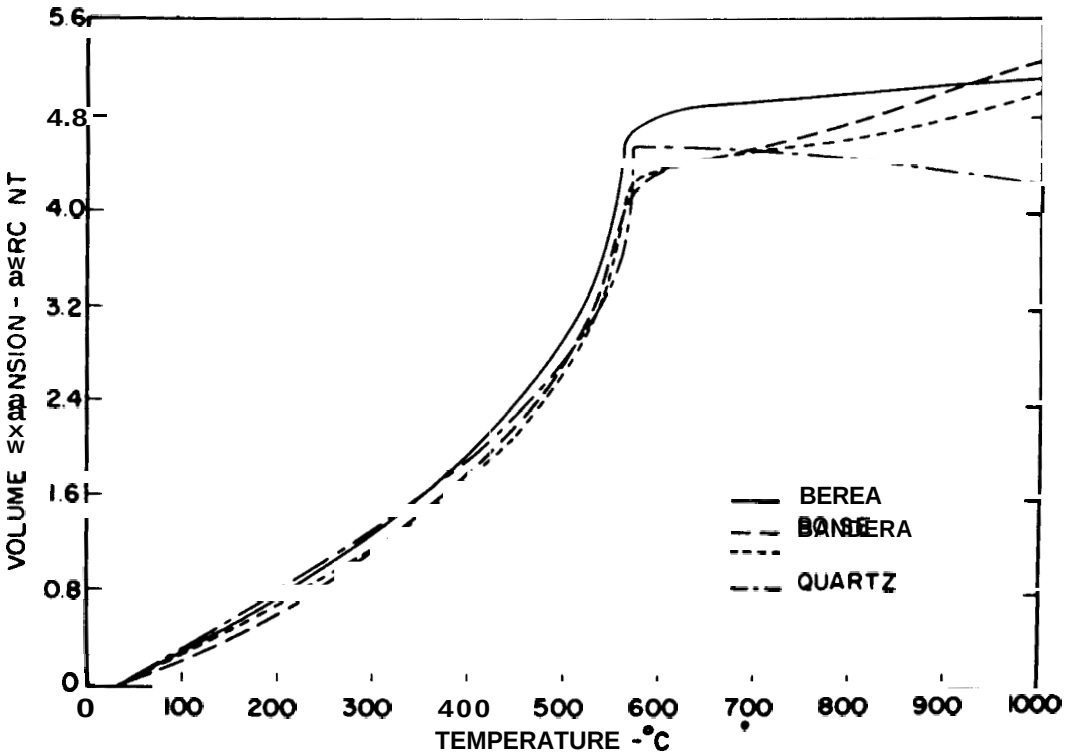

FIGURE 9 — VOLUME EXPANSION OF SANDSTONES.
(Ref. 12)

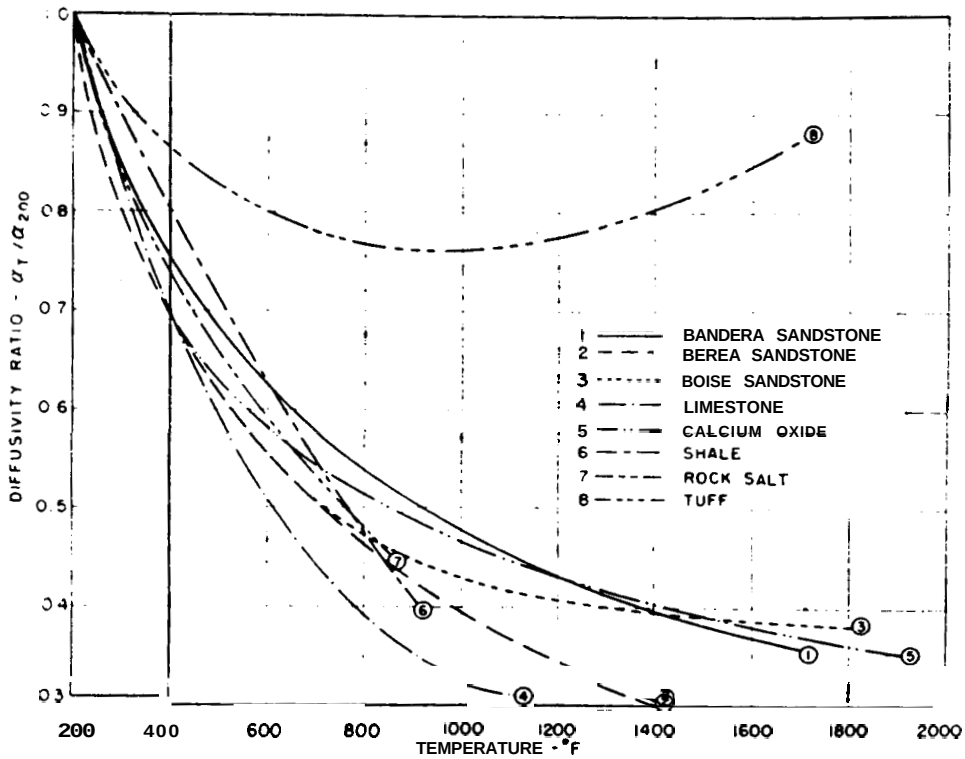

FIGURE 10 —THERMAL DIFFUSIVITY RATIO, INITIAL RUNS.
(Ref. 13)

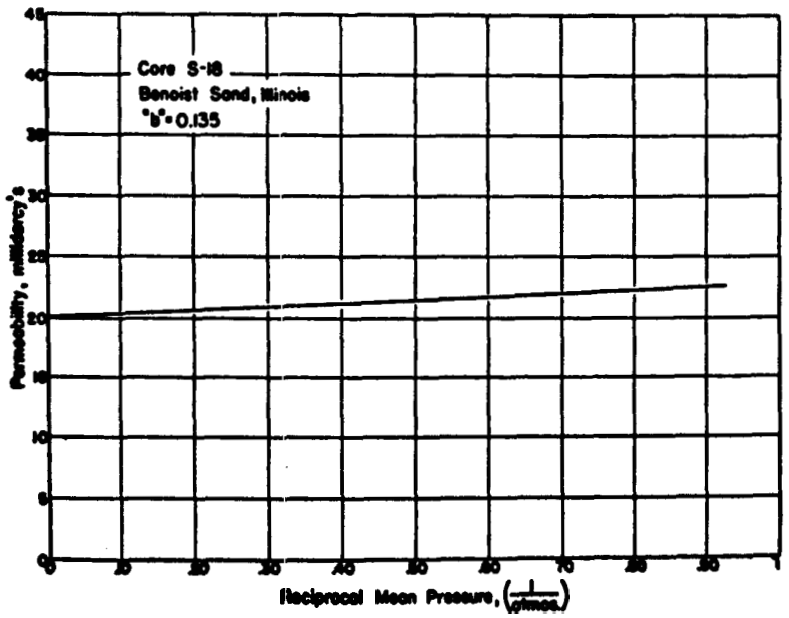

FIG. 5

FIGURE 11 **Relationship between the Permeability to Gas and the Mean Pressure at which Gas Flows through a Medium, a Relationship Making Possible the Determination of the Permeability of the Medium to a Non-Reacting Liquid**

(from API RP 27, Am. Petr. Inst., Aug. 1956)

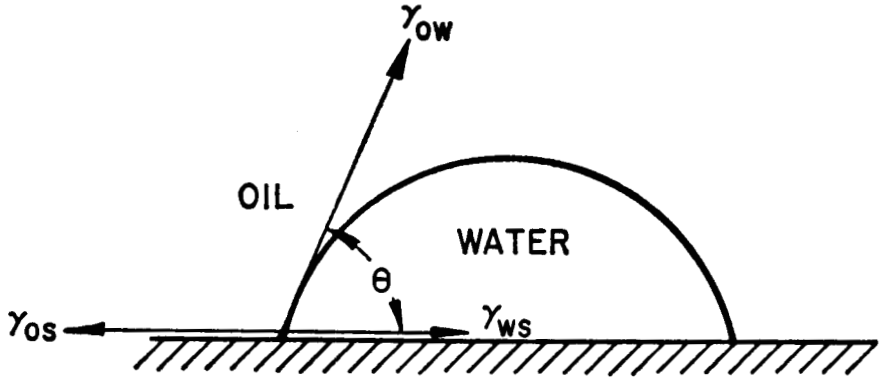

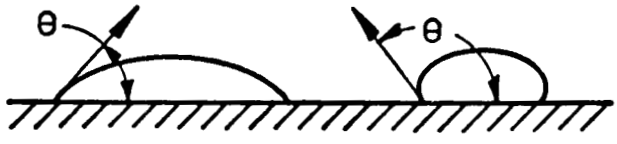

FIGURE 12 **Relationship between preferential wetting and contact angle.** (Ref. 15)

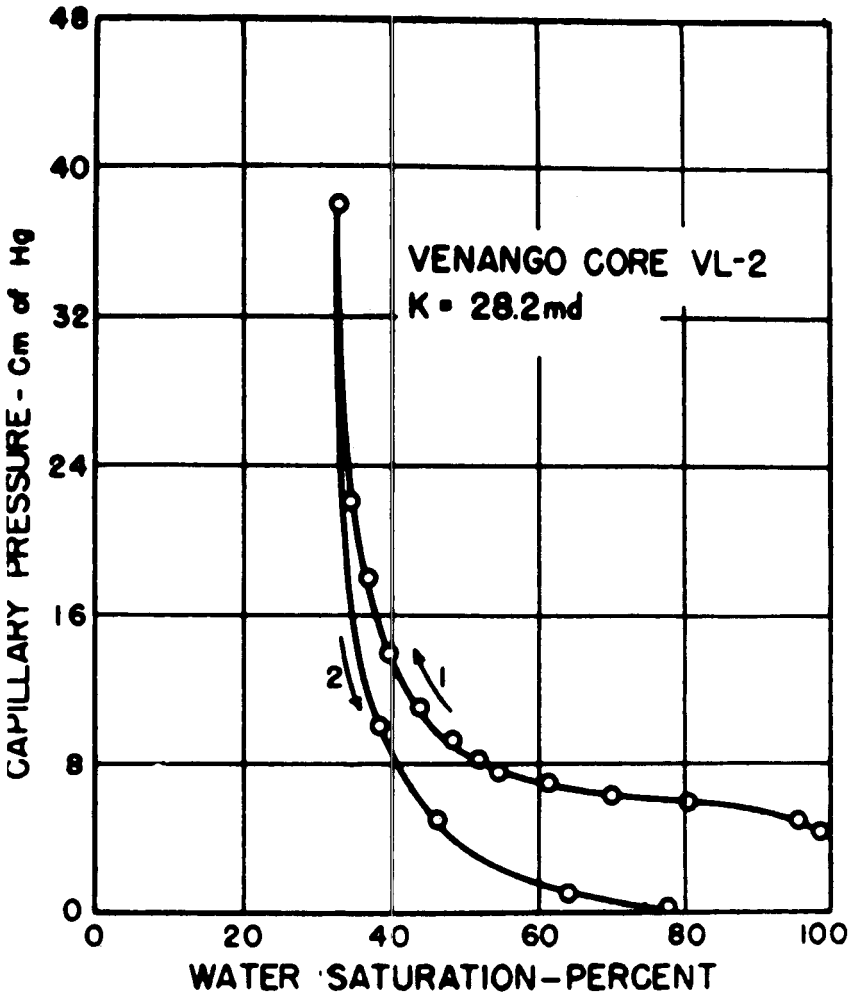

FIGURE 13 —Capillary pressure vs. water saturation.

(Ref. 16)

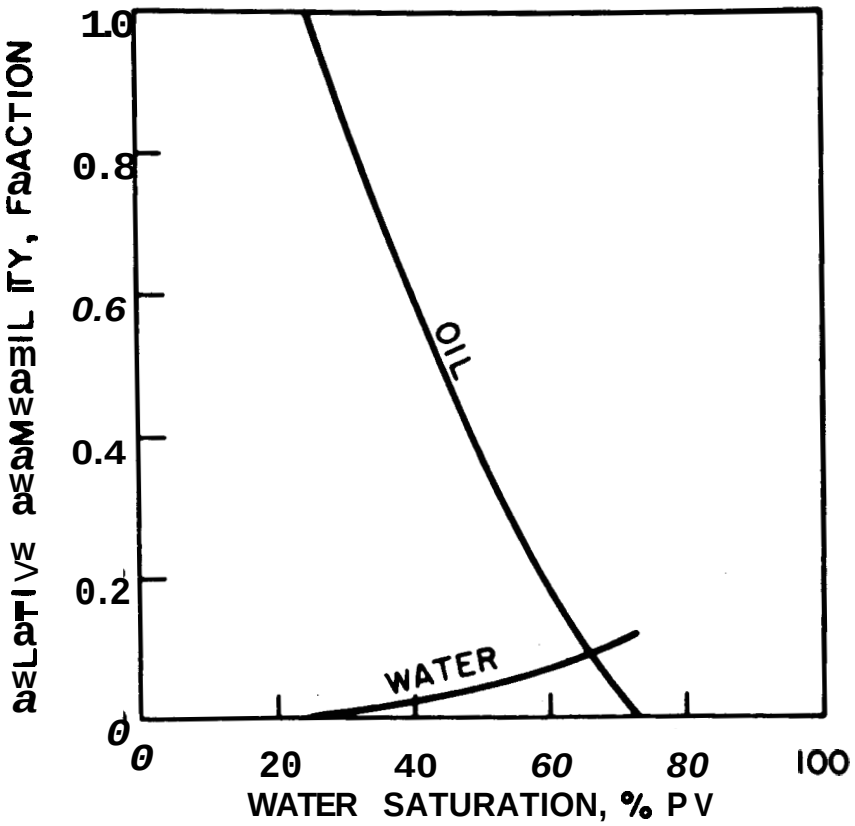

FIGURE 14 Typical water-oil relative permeability characteristics. strongly water-wet rock. (Ref. 17)

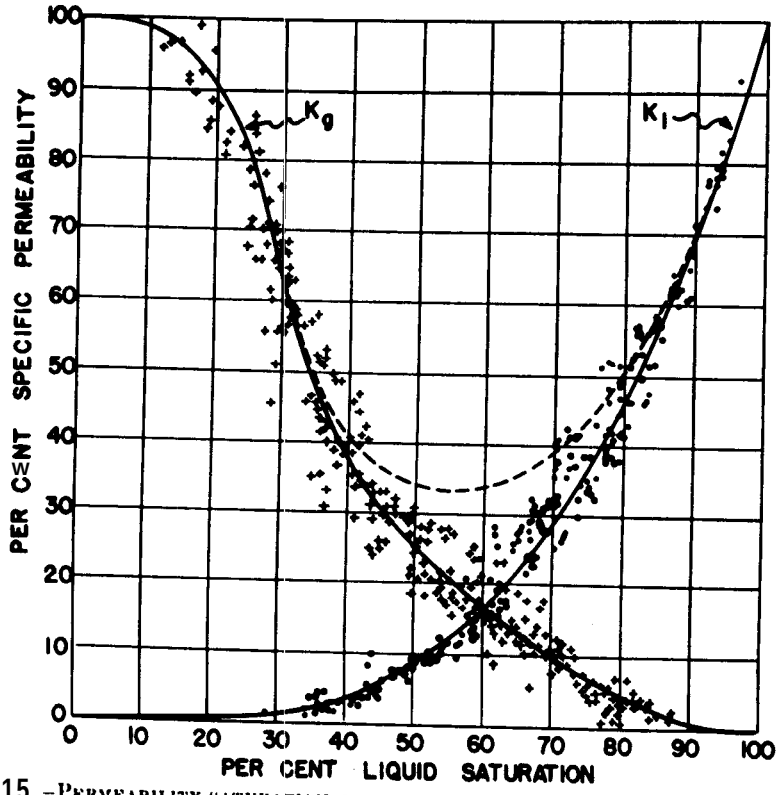

FIGURE 15 –PERMEABILITY-SATURATION DATA FOR FOUR DIFFERENT SANDS, INCLUDING THOSE OF FIGS. 4 AND 5.

(Ref. 18)

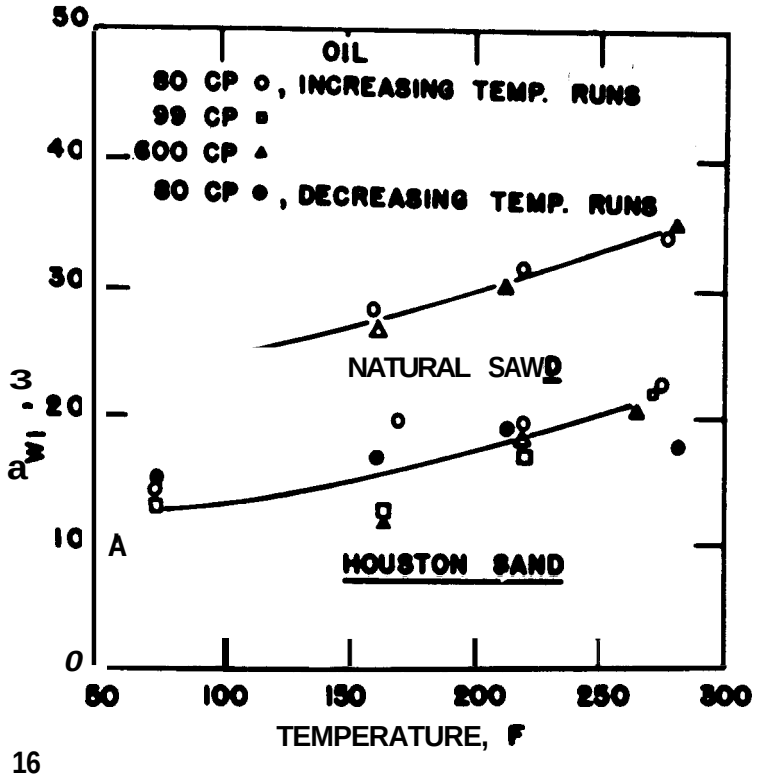

FIGURE 16 IRREDUCIBLE WATER SATURATION VS TEMPERATUREFORHOUSTONSANDANDNATURAL SAND. (Ref. 19)

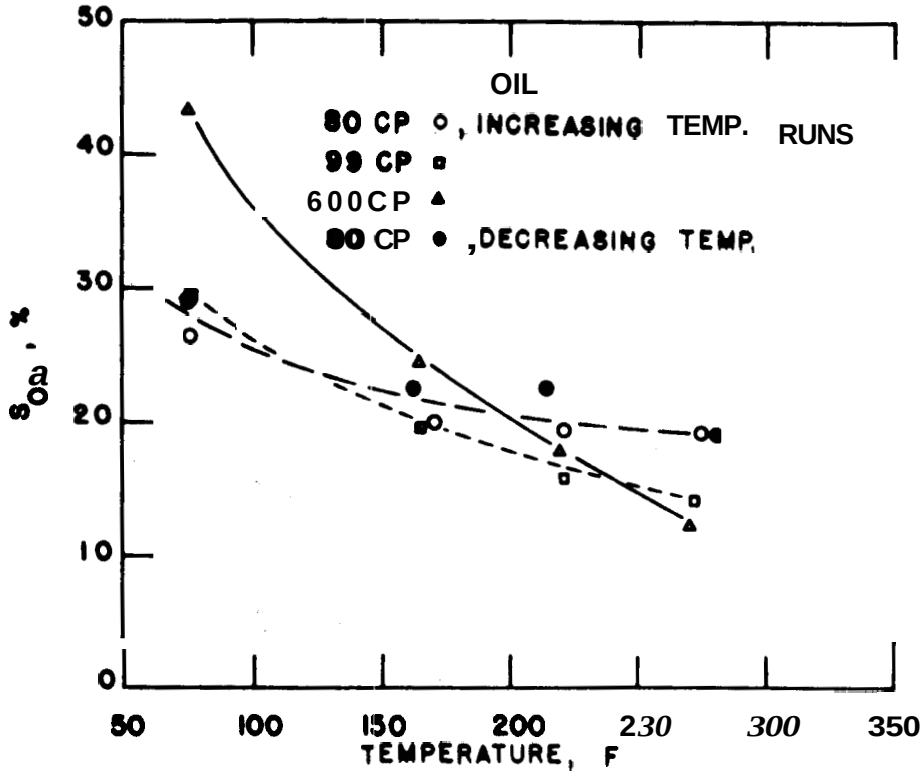

FIGURE 17 **RESIDUAL OIL SATURATION VS TEMPERATURE FOR HOUSTON SAND.** (Ref. 19)

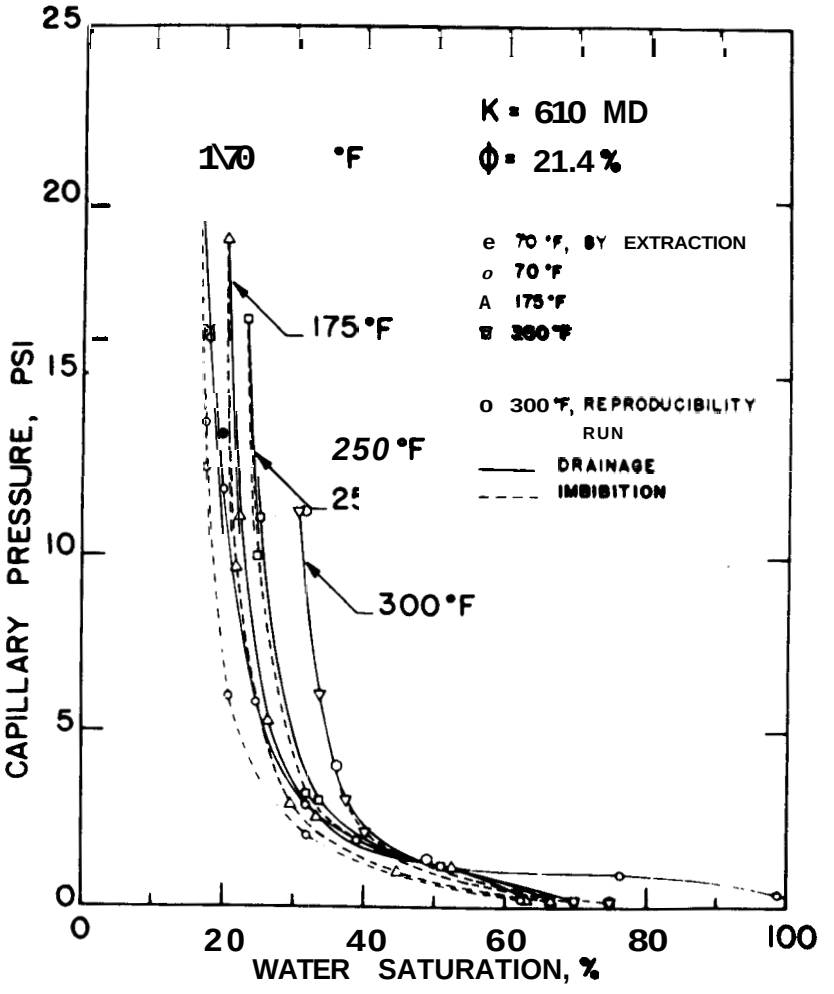

FIGURE 18 **Capillary pressure vs water saturation for Berea sandstone core A.** (Ref. 20)

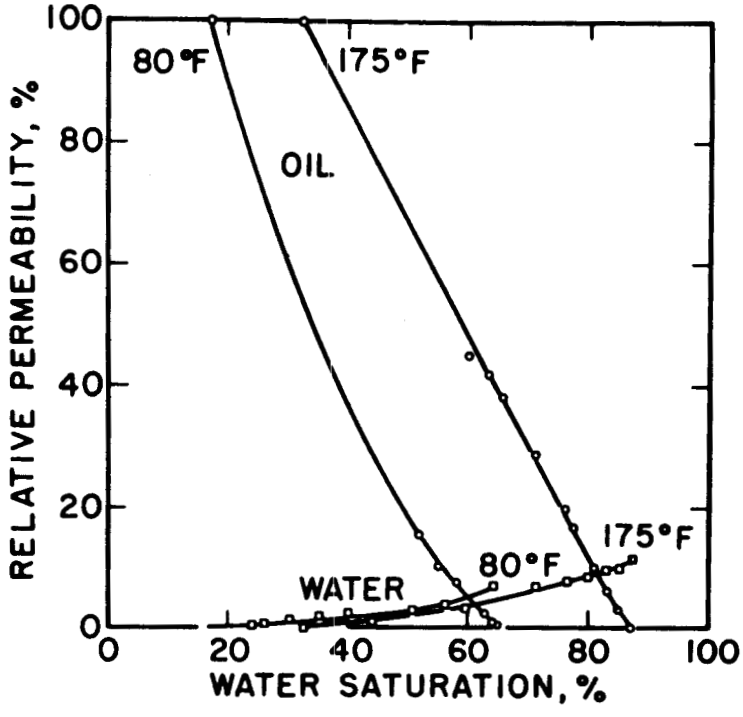

FIGURE 19

Individual relative permeabilities as a function of temperature; Core 4, Boise sandstone. **(Ref. 21)**

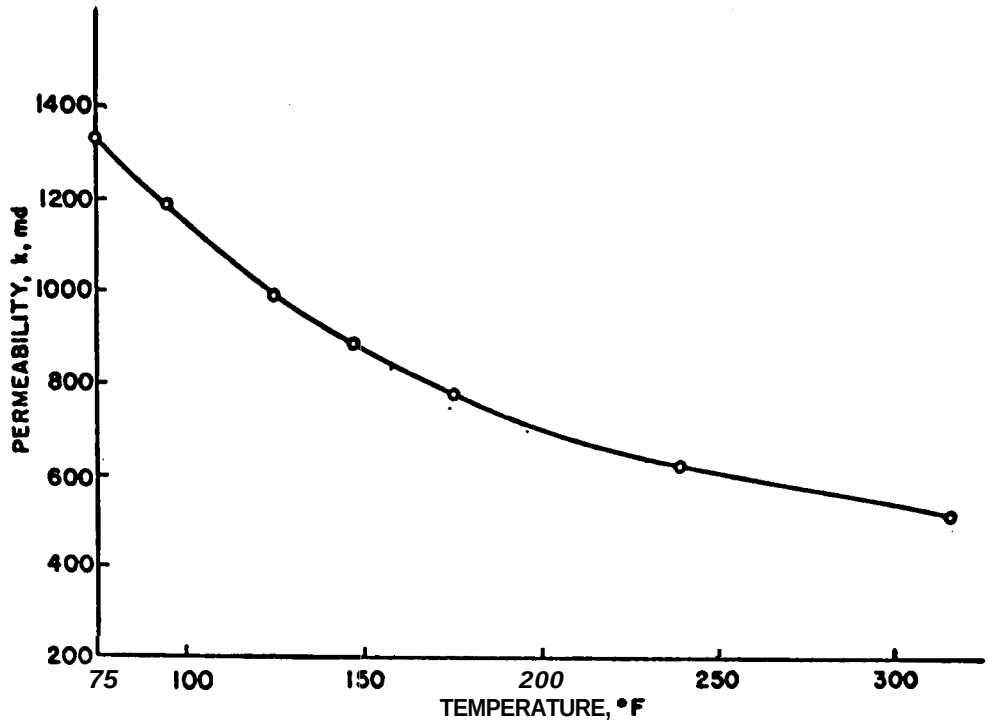

FIGURE 20 EFFECT OF TEMPERATURE ON ABSOLUTE PERMEABILITY OF BOISE SANDSTONE; CORE NUMBER 7 (Ref. 21)

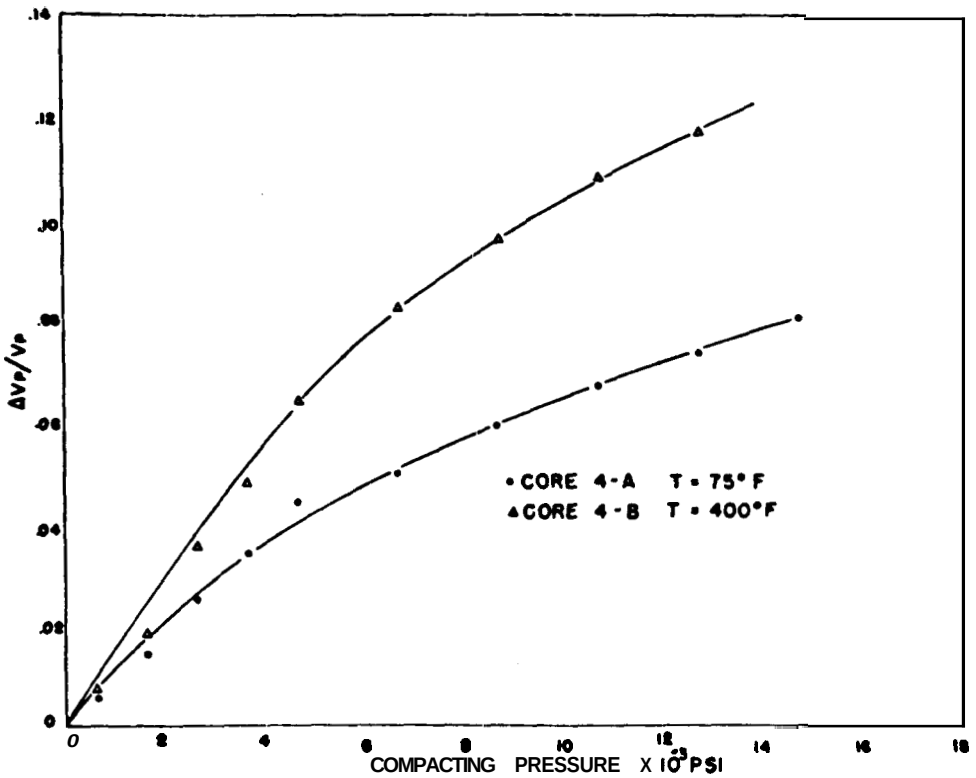

FIGURE 21 - Change in cumulative fractional pore volume with pressure core 4 at 75 and 400°F. **(Ref.** 24)

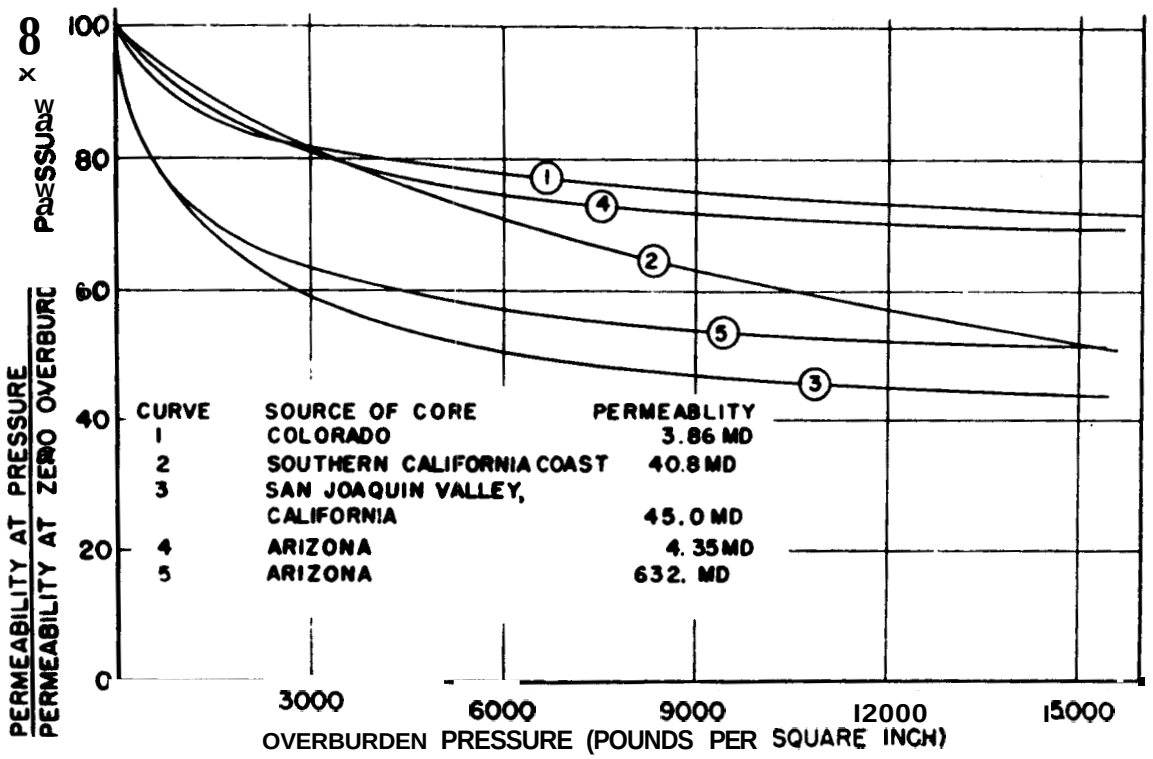

FIGURE 22 CHANGE IN PERMEABILITY WITH OVERBURDEN PRESSURE.

(Ref. *26*)

FIGURE 23

PRESSURE-TEMPERATURE DIAGRAM FOR WATER

(Ref. 38)

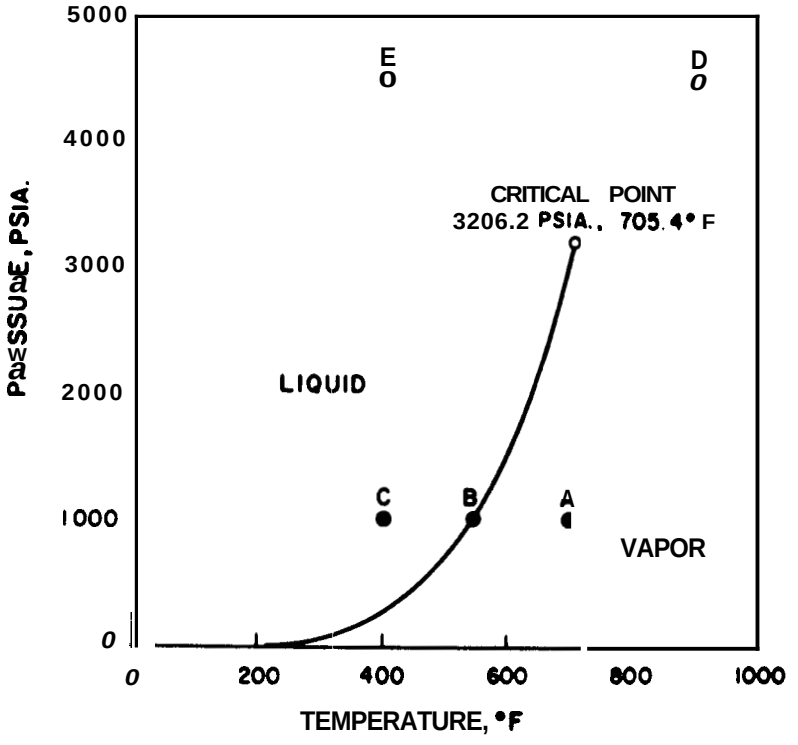

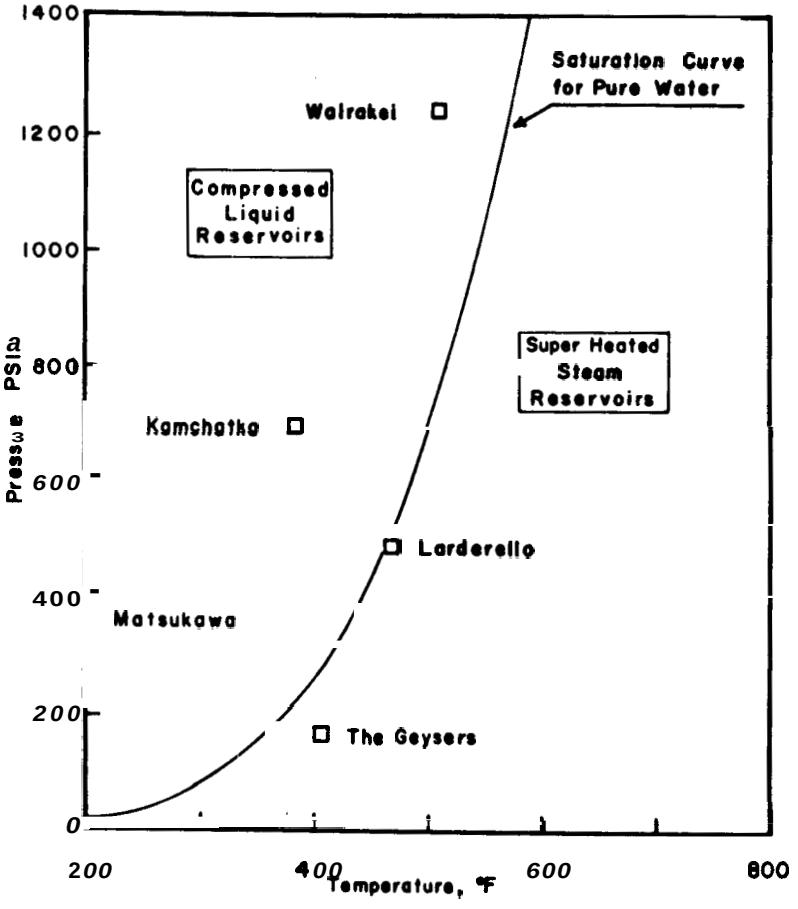

FIGURE 24 Reservoir temperature and pressure data for geothermal reservoirs

(Ref. 60)

FIGURE 25

PRESSURE–SPECIFIC VOLUME CHART FOR WATER

(Ref. 38)

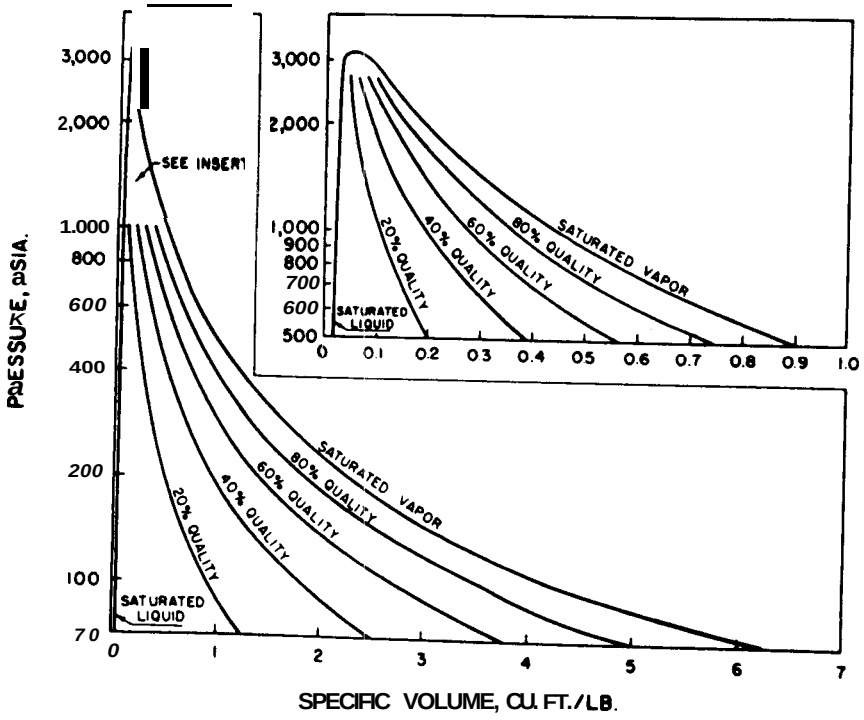

FIGURE 26

PRESSURE – ENTHALPY DIAGRAM FOR WATER

(Ref. 38)

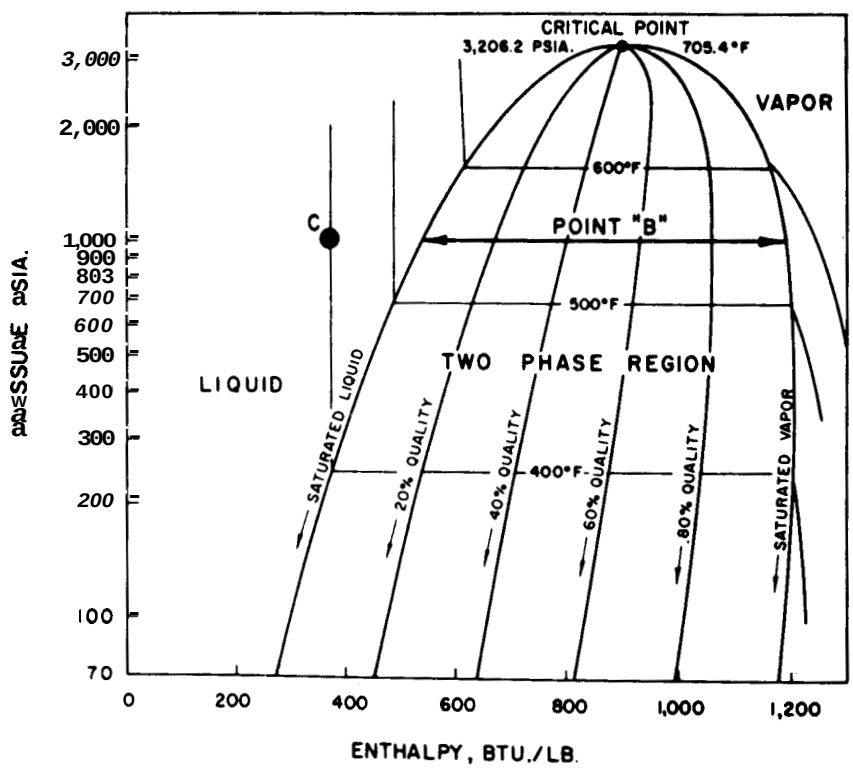

FIGURE 27

Viscosity of Saturated Water and Steam

(modified from Ref. 38)

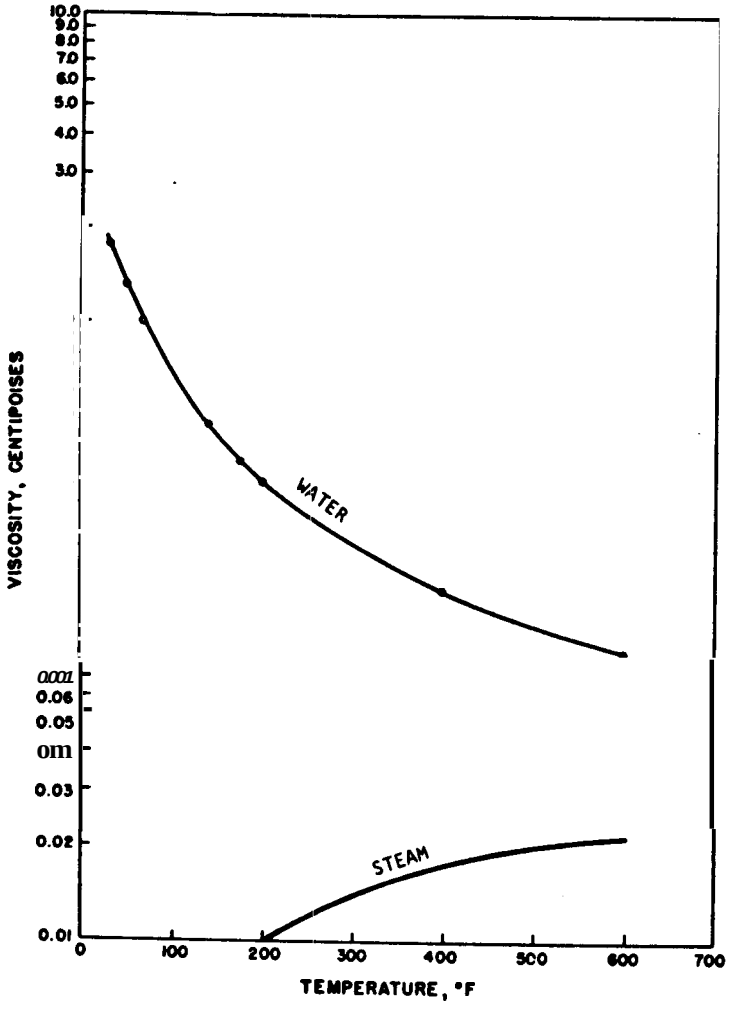

IT

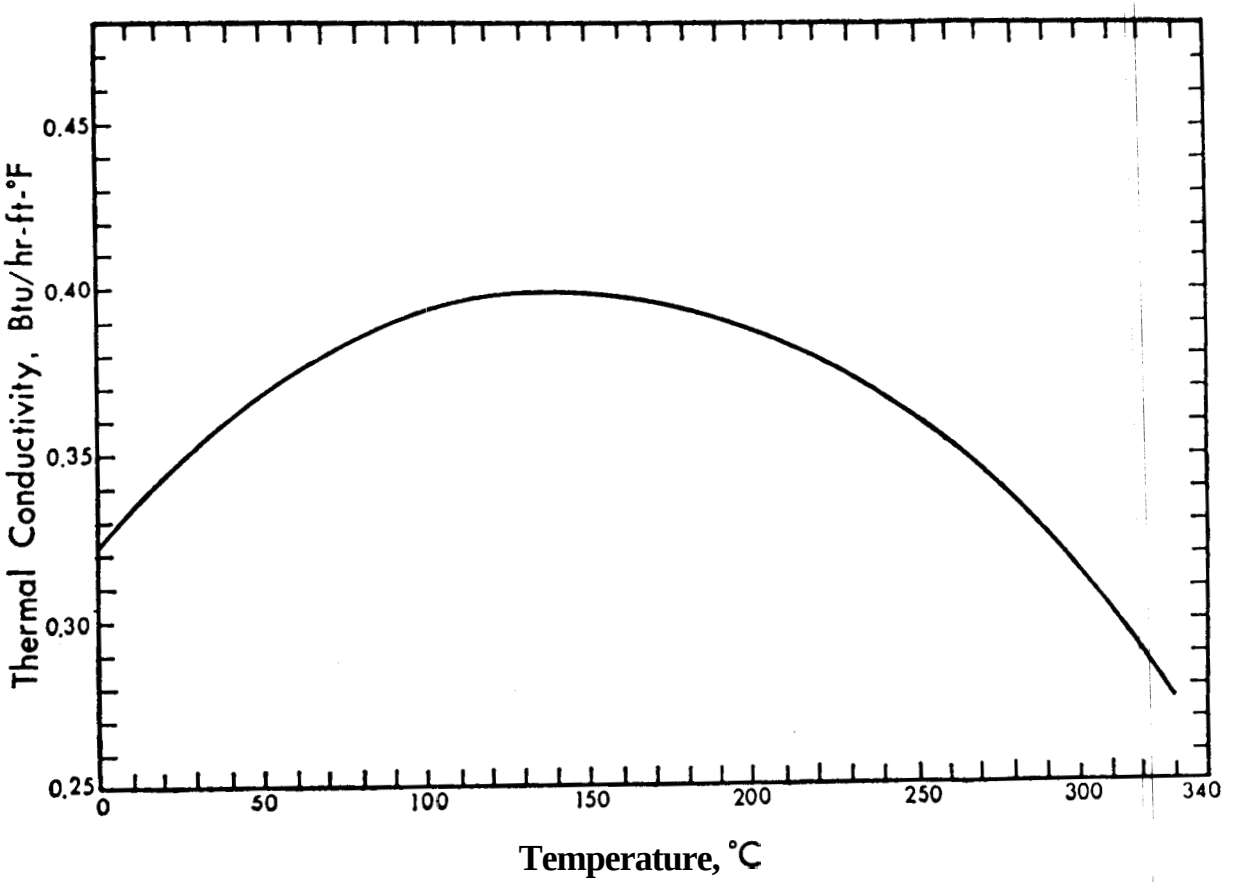

FIGURE 28. THE THERMAL CONDUCTIVITY OF SATURATED LIQUID WATER (Ref. 39)

FIGURE 29

FORMATION VOLUME FACTOR FOR PURE LIQUID WATER AS A FUNCTION OF PRESSURE AND TEMPERATURE

(Ref. 38)

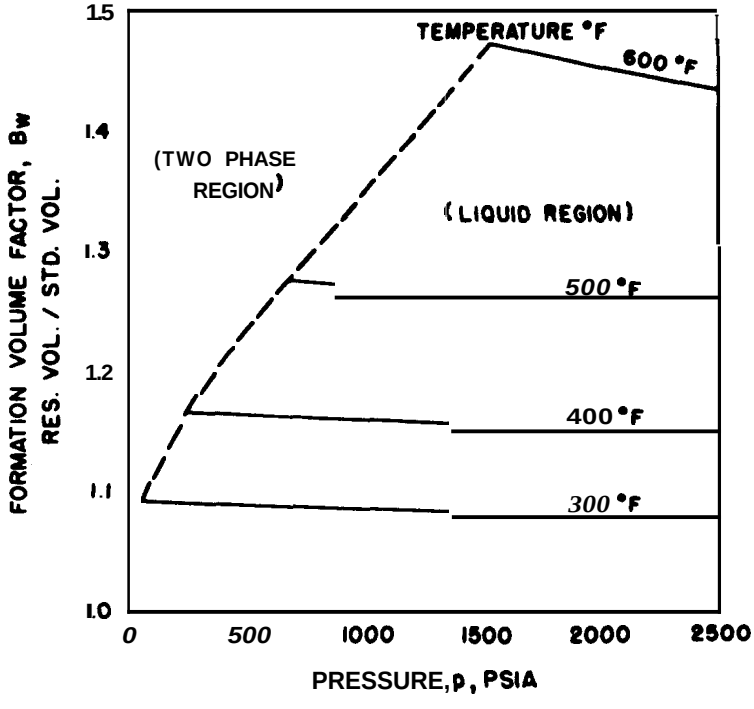

FIGURE 30

PRESSURE - SPECIFIC VOLUME CHART FOR SUPERHEATED STEAM

(Ref. 38)

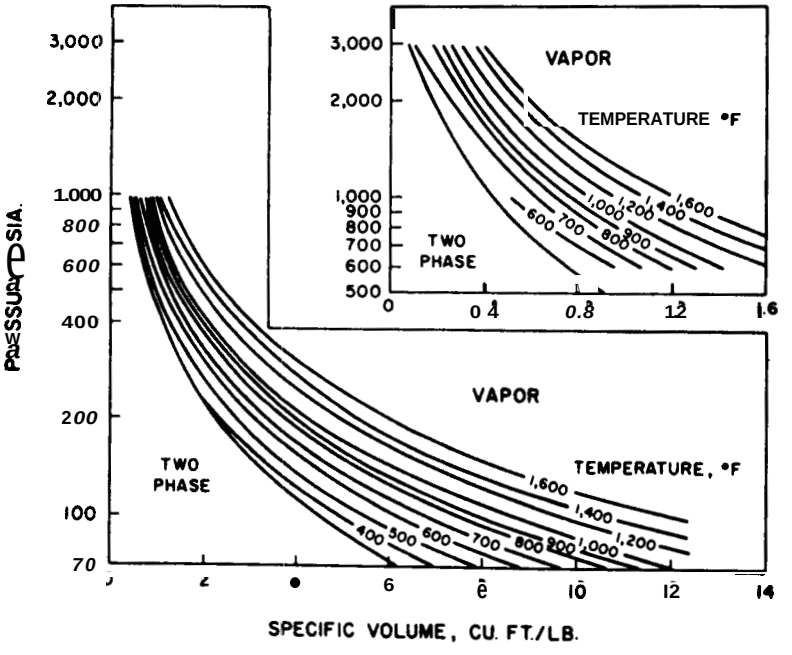

FIGURE 31
GAS LAW DEVIATION FACTOR FOR STEAM (Ref. 63)

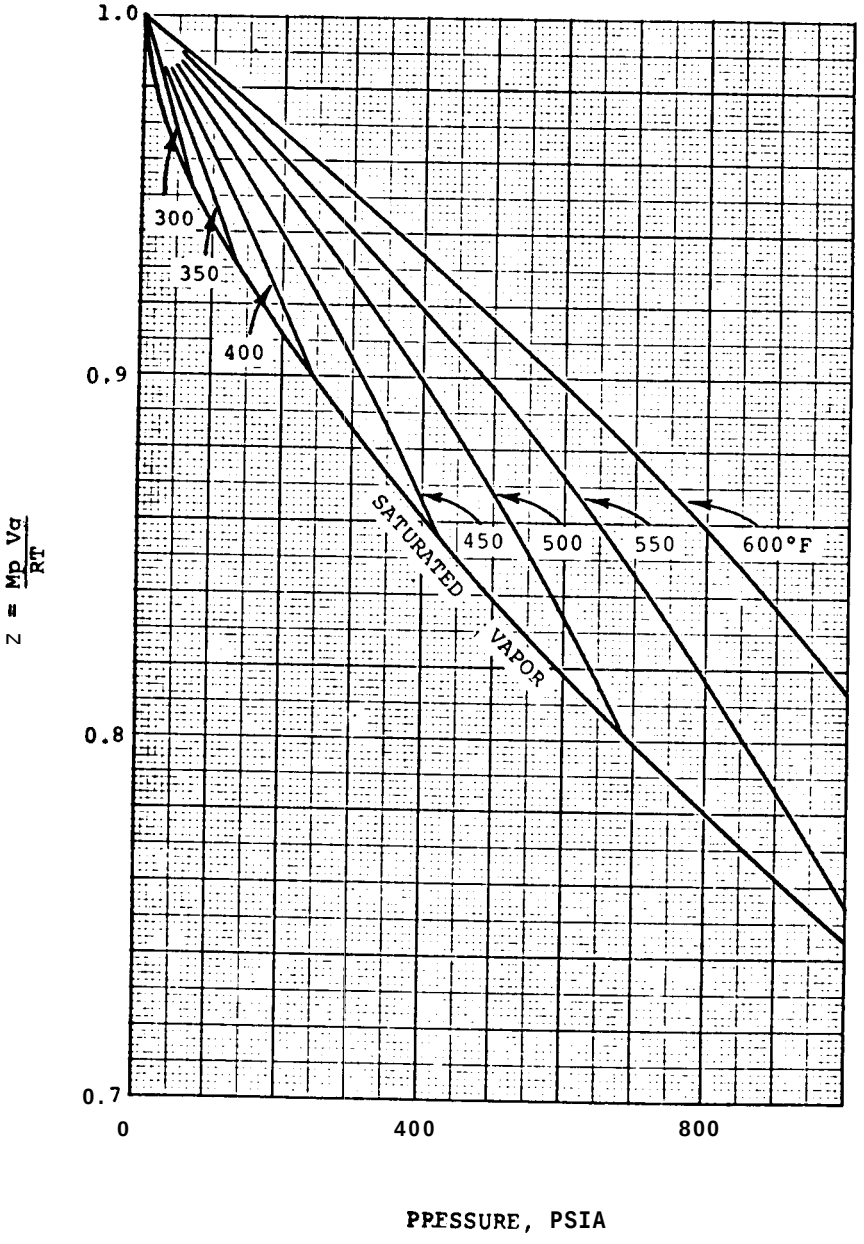

FIGURE 32

PRESSURE - ENTHALPY DIAGRAM FOR SUPERHEATED STEAM

(Ref. 38)

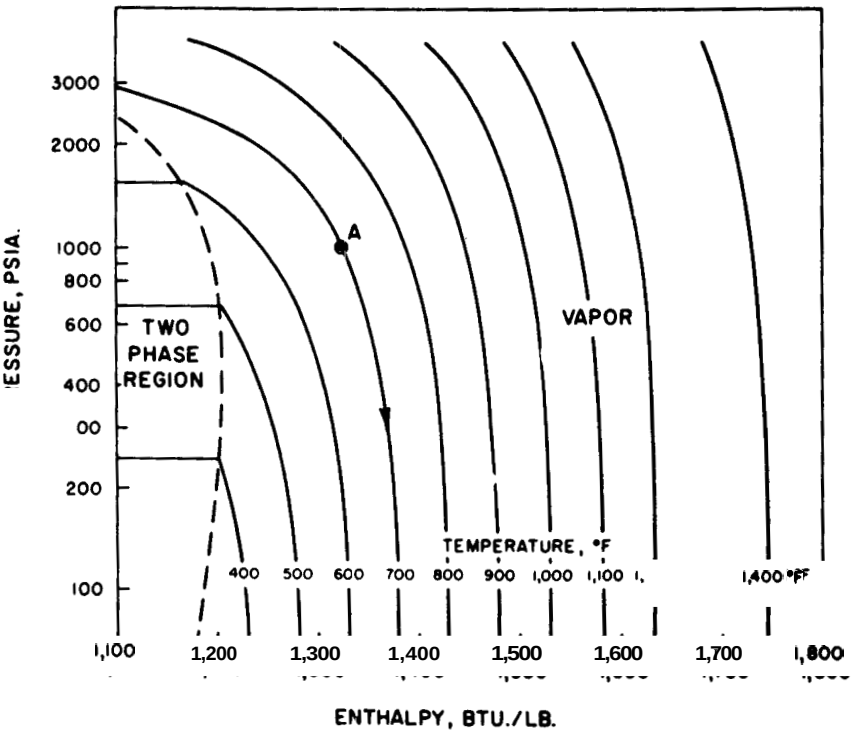

REFERENCES

1. Birch, Francis and Clark, Harry: "The Thermal Conductivity of Rocks and Its Dependence upon Temperature and Composition, Part I", *Am.* J. Science, 238, No. 8 (Aug. 1940), pp. 529–558.
2. Birch, Francis and Clark, Harry: "The Thermal Conductivity of Rocks and Its Dependence upon Temperature and Composition, Part II", Am. J. Science, 238, No. 9 (Sept. 1940), pp. 613–635.
3. Somerton, Wilbur H. : "Some Thermal Characteristics of Porous Rocks," Trans. AIME, 213 (1958), pp. 375-378.
4. Kunii, D. and Smith, J. M.: "Thermal Conductivities of Porous Rocks Filled with Stagnant Fluid," Soc. Pet. Engr. J. (Mar. 1961), pp. 37–42.
5. Adivarahou, P., Kunii, D. and Smith, J. M.: "Heat Transfer in Porous Rocks Through Which Single–phase Fluids Are Flowing," Soc. Pet. Engr. J. (Sept. 1962), pp. 2'90–296.
6. Willhite, G. P., Dranoff, J. S. and Smith, J. M.: "Heat Transfer Perpendicular to Fluid Flow .in Porous Rocks," Soc. Pet. Engr. J. (Sept. 1963), pp. 185–188.
7. Anand, J., Somerton, W. H. and Gomaa, E.: "Prediction of Thermal Properties of Formations from Other Known Properties," Paper No.' SPE–4171, 43rd California Regional Meeting, SPE of AIME, Bakersfield, Calif., Nov. 8–10, 1972.
8. Tikhomirov, V. M.: "Conductivity of Rocks and Their Relationship with Density, Saturation and Temperature," Neftianoe Khoziaistro (in Russian), 46, No. 4 (1968), p. 36.
9. Gomaa, Ezzat E. and Somerton,, W. H.: "Thermal Behavior of Multifluid-Saturated Formations, Part I: Effect of Wettability, Saturation and Grain Structure," Paper No. SPE 4896–A, 44th California Regional Meeting, SPE of AIME, San Francisco, Calif., April 4–5, 1974.
10. Gomaa, Ezzat E. and Somerton, W. H.: "Thermal Behavior of Multifluid–Saturated Formations, Part II: Effect of Vapor Saturation - Heat Pipe Concept and Apparent Thermal Conductivity," Paper No. SPE 4896–B, 44th California Regional Weeting, SPE of AIME, San Francisco, Calif., April 4–5, 1974.
11. Martin, W. L. and Dew, J. N.: "How to Calculate Air Requirements for Forward Combustion," Petroleum Engineer (Dec. 1964 and Feb. 1965).
12. Somerton, W. H. and Selim, M. A.: "Additional Thermal Data for Porous Rocks - Thermal Expansion and Heat of Reaction," Soc. Pet. Engr. J. (Dec. 1961), pp. 249–253.
13. Somerton, W. H. and Boozer, G. D.: "Thermal Characteristics of Porous Rocks at Elevated Temperatures," Trans. AIME, 219 (1960), pp. 418–422.
14. Klinkenberg, L. J.: "The Permeability of Porous Media to Liquids and Gases," Drilling and Production Practice (1941), pp. 200–213.

15. Raza, S. H., Treiber, L. E., and Archer. D. L.: "Wettability of Reservoir Rocks and Its Evaluation," Prod. Monthly (April 1968), 32, No. 4, pp. 2–7.

16. Killins, C. R., Nielsen, R. F. and Calhoun, J. C.: "Capillary Desaturation and Imbibition in Porous Rocks," Prod. Monthly (Dec. 1953) 18, No. 2, pp. 30–39.

17. Craig, F. F., Jr.: The Reservoir Engineering Aspects of Waterflooding, SPE Monograph, Vol. 3.

18. Muskat, M., Wyckoff, R. D., Botset, H. G. and Meres, M. W.: "Flow of Gas–liquid Mixtures through Sands," Trans., AIME (1937), 123, pp. 69–96.

19. Poston, S. W., Ysrael, S., Hossain, A. K. M. S., Montgomery, E. F. IV and Ramey, H. J., Jr.: "The Effect of Temperature on Irreducible Water Saturation and Relative Permeability of Unconsolidated Sands," Soc. Pet. Engr. J. (June 1970), pp. 171–180.

20. Sinnokrot, A. A., Ramey, H. J., Jr. and Marsden, S. S.: "Effect of Temperature Level upon Capillary Pressure Curves," Paper No. SPE 2517, presented at the 44th Annual SPE Fall Meeting, Denver, Colo., Sept. 28-Oct. 1, 1969.

21. Weinbrandt, R. M., Ramey, H. J., Jr. and Cassé, F.: "The Effect of Temperature on Relative Permeability of Consolidated Rocks," Paper No. SPE 4142, presented at the 47th Annual SPE Fall Meeting, San Antonio, Texas, Oct. 8–11, 1972.

22. Afinogenov, Y. A.: "How the Liquid Permeability of Rocks Is Affected by Pressure and Temperature," SNIGGIMS (1969), No. 6, pp. 34–42 (translation from Consultants Bureau, 227 W. 17 St., New York, NY 10011).

23. Lo, H. Y. and Mungan, N.: "Effect of Temperature on Water–Oil Relative Permeabilities in Oil–Wet and Water–Wet Systems," Paper No. SPE 4505, presented at the 48th Annual SPE Fall Meeting, Las Vegas, Nevada, Sept. 30-Oct. 3, 1973.

24. Von Gonten, W. D. and Choudhary, B. K.: "The Effect of Pressure and Temperature on Pore Volume Compressibility," Paper No. SPE 2526, presented at the 44th Annual SPE Fall Meeting, Denver, Colorado, Sept. 28-Oct. 1, 1969.

25. Zoback, M. D. and Byerlee, J. D.: "Permeability, Compressibility and Effective Stress," unpublished report (Feb. 1974).

26. Fatt, I. and Davis, D. H.: "Reduction in Permeability with Overburden Pressure," Trans., AIME (1952), 195, 329.

27. Wyble, D. O.: "Effect of Applied Pressure on the Conductivity, Porosity and Permeability of Sandstones," Trans., AIME (1958), 213, pp. 430–432.

28. Dobrynin, V. M.: "Effect of Overburden Pressure on Some Properties of Sandstones," Soc. Pet. Engr. J. (Dec. 1962) 2, No. 4, pp. 360–366.

29. Gray, D. H., Fatt, I. and Bergamini, G.: "The Effect of Stress on Permeability of Sandstone Cores," Soc. Pet. Engr. J. (June 1963), pp. 95–100.

30. Wilhelmi, B. and Somerton, W. H.: "Simultaneous Measurement of Pore and Elastic Properties of Rocks under Triaxial Stress Conditions," Paper No. SPE 1706 (1967).

31. Krauskopf, K. B.: Introduction to Geochemistry, McGraw-Hill, New York, NY, 1967.

32. Butler, J. N.: Solubility and pH Calculations, Addison-Wesley, Palo Alto, CA, 1964.

33. White, E. E.: "Geochemistry Applied to the Discovery, Evaluation and Exploitation of Geothermal Energy Resources," Geothermics, Special Issue 2, Proc. of U. N. Symposium on the Development and Utilization of Geothermal Resources, Pisa, 1970, Vol. 1.

34. Fournier, R. O. and Truesdell, A. H.: "Chemical Indications of Subsurface Temperature Applied to Hot Spring Waters of Yellowstone National Park, Wyoming, U.S.A.", Geothermics, Special Issue 2, Proc. of U. N. Symposium on the Development and Utilization of Geothermal Resources, Pisa, 1970, Vol. 2, Part 1.

35. Keenan, J. H. and Keyes, F. G.: Thermodynamic Properties of Steam, John Wiley and Sons, Inc., New York, NY, 1936.

36. Meyer, C. A., McClintock, R. B., Silvestri, G. J. and Spencer, R. C., Jr.: 1967 ASME Steam Tables, Am. Soc. Hech. Engrs., 2nd ed., New York, NY, 1968.

37. Keenan, J. H., Keyes, F. G., Hill, P. G. and Moore, J. G.: Steam Tables: Thermodynamic Properties of Water Including Vapor, Liquid and Solid Phases (English Units), John Wiley and Sons, Inc., New York, NY, 1969.

38. Whiting, R. L. and Ramey, H. J., Jr.: "Application of Material and Energy Balances to Geothermal Steam Production," J. Pet. Tech. (July 1969), pp. 893-900.

39. Farouq Ali, S. M.: Oil Recovery by Steam Injection, Producers Pub. Co., Bradford, PA, 1970.

40. Calhoun, J. C., Lewis, M., Jr. and Newman, R. C.: "Experiments on the Capillary Properties of Porous Solids;" Trans. AIME, 186 (1949), pp. 189-196.

41. Edlefsen, N. E. and Anderson, A. B. C.: "Thermodynamics of Soil Moisture," Hilgardia, Calif. Agricultural Exp. Station, Univ. of Calif. at Berkeley, 15, No. 2 (Feb. 1943), p. 31.

42. Cady, G. V., Bilhartz, H. L., Jr. and Ramey, H. J., Jr.: "Model Studies of Geothermal Steam Production," Water 1972, AIChE Symposium Series (1973).

43. Amyx, J. W., Bass, D. M., Jr. and Whiting, R. L.: Petroleum Reservoir Engineering, McGraw-Hill, New York, NY, 1960.

44. Dodson, C. R. and Standing, M. B.: "Pressure-Volume-Temperature and Solubility Relations to Natural Gas-Water Mixtures," API Drilling and Production Practice, American Petroleum Institute, 1944.

45. Rowe, W. E.: "Effect of Salinity on Physical Properties of Water," Secondary Recovery of Oil in the United States, American Petroleum Institute, 1950.

46. Beal, Carlton: "The Viscosity of Air, Water, Natural Gas, Crude Oil and Its Associated Gases at Oil Field Temperatures and Pressures," Trans., AIME, 165 (1946).

47. Bridgman, D. W.: The Physics of High Pressure, McMillan Co., New York, NY, 1931.

48. Long, G. and Chierici,, G. L.: "Compressibilite et Masse Specifique des Eaux de Gisement dans les Conditions des Gisements, Application a Quelque Problemes de 'Reservoir Engineering"' presented at Fifth World Petroleum Congress, 1959.

49. Van Wingen, N.: "Viscosity of Oil, Water, Natural Gas, and Crude Oil at Varying Pressures and Temperatures," Secondary Recovery of Oil in the United States, American Petroleum Institute, 1950.

50. Stanley, E. M. and Batten, R. C.: "Viscosity of Sea Water at Moderate Temperatures and Pressures," J. Geophys. Res., 74, No. 13 (June 20, 1969), pp. 3415–3420.

51. Eilerts, C. L., Carlson, H. A. and Mullens, N. B.: "Effect of Added Nitrogen on Compressibility of Natural Gas," World Oil (June–July 1948).

52. Olds, R. H., Sage, B. H. and Lacey, W. N.: "Partial Volumetric Behavior of the Methane–Carbon Dioxide System," Fundamental Research on the Occurrence and Recovery of Petroleum, American Petroleum Institute, 1943.

53. Reamer, H. H., Sage, B. H. and Lacey, W. N.: "Volumetric Behavior of Hydrogen Sulfide," Ind. Engr. Chem, 42, No. 1 (Jan. 1950), p. 140.

54. Herning, F. and Zipperer, L.: "Calculation of the Viscosity of Technical Gas Mixtures from the Viscosity of the Individual Gases," Gas–U. Wasserfach, 79 (1936).

55. Weast, R. C.: Handbook of Chemistry and Physics, The Chemical Rubber Co., Ohio, 48th ed. (1967-68).

56. Strobel, C. J.: Model Studies of Geothermal Fluids Production from Consolidated Porous Media," Engineer's thesis, Stanford Univ., July 1973,

57. Kuhn, C. S. and Koch, R. L.: "In–Situ Combusion," Oil & Gas J. (Aug. 10, 1953), *52*, No. 14, p. 96.

58. Stovall, S. L.: "Recovery of Oil from Depleted Sands by Means of Dry Steam," Oil Weekly (Aug. 13, 1934), 74, p. 17.

59. Gates, C. S. and Ramey,, H. J., Jr.: "Field Results of South Bebridge Thermal Recovery Experiment," Trans., AIME (1958), 213, p. 236.

60. Cady, G. V. : "Model Studies of Geothermal Fluid Production," Ph.D. dissertation, Stanford Univ., Nov. 1969.

61. Rowe, A. M., Jr. : "Thermodynamics Applied to Reservoir Engineering," Course'notes for Petroleum Engineering 273, Winter 1973–74, Stanford Univ,

62. Helgeson, H. C.: "Thermodynamics of Hydrothermal Systems at Elevated Temperatures and Pressures," *Am.* J. Science, 267, Summer 1969, pp. 729–804.

63. Ramey, H. J., Jr.: A Reservoir Engineering Study of the Geysers Geothermal Field, 1968; submitted as evidence, Reich and Reich: Petitioners vs. Commissioner of Internal Revenue, 1969 Tax Court of the United States, 52. T.C. No. 74, 1970.

Discussion Following Ramey Paper

Rinehart

Do you think these things would hold for large, fractured mass when you have microscopic fractures with impermeable rock in between?

Ramey

In some cases we already know that they do. There are many oil and gas reservoirs that are in fact large, fractured masses. Generally speaking, the laws of nature seem to work the same there. Now some of the details on these homogeneous porous structures, the relative permeability curve details, would not be identically the same. It has amazed me to find that some of the massive, fractured reservoirs seem to follow simple mechanics.

Oki

The permeability is a function of temperature. When the temperature is increased, the permeability becomes lower; then when the temperature is reduced, the original numerical value for permeability is reached. I mean it is almost reversible.

Ramey

It is reversible. One other thing: the shapes of the curves, whether it's temperature or pressure, are almost the same. In data where permeability ratio is plotted versus effective pressure, you will note that the shape is almost identical with what you get for temperature, In our temperature work we have kept the confining pressure constant, just varying the temperature in the system, and we see this reversible result. In our data it is perhaps not totally reversible; it will move down the line and come back up slightly below its original path. But the difference is not much. Within the experimental accuracy it appears to be reversible. On the other work, on relative permeability, most of it does seem to be temperature level reversible. If you heat a core and measure relative permeability you get one value; if you cool it off and heat it up again you get the same value.

Rinehart

These are all corrected for viscosity?

Ramey

Yes.

Rinehart

Do you feel that your correction is good?

Ramey

We know it is. We've used fluids where the density of the fluid is known perfectly, we've used desensitized cores where we're not getting reaction with the core material, we've tested the fluids before and after, we've measured everything we can think of to be sure nothing has changed,

Coryell

It looks as though you are drawing attention to a large body of empirical evidence for temperature dependence of these parameters, Would you care to comment as to how you see the future, where the science is going to go, the state of the theory at the present time?

Ramey

Yes, you see a lot of interesting problems,

Coryell

You see a lot of interesting behavior, but is there the science and the basic understanding of why it's happening?

Ramey

Oh, very definitely. Everything I have shown you, I can explain I should have added that this one is almost on the forefront of knowledge and I can tell you what I think is the cause. In many cases, for example, the change in thermal conductivity with temperature will fit a very logical model of this system to the point that you can almost calculate the results you will get. Practically everything that has been done has been strongly related to underlying principles. People have been searching for ways to compute the result. Generally speaking, we have wanted this so we could patch it into some computer software and forecast what would happen under different cases. It's been necessary to generalize; it's been necessary to, at least, curve-fit to the point that is accessible to a computer. Almost everything that exists in the literature will have a very good explanation; it is not empirical. These are experimental determinations, of course; when you deal in this area, what you are talking about are experimental measurements that fit your constants. But the laws of physics still apply.

What I really deal in are reservoir models, physical models. We produce an oil reservoir, measure pressure all over it--what comes out, what goes in--and I attempt to build some mathematical picture of the thing so I can forecast what will happen under any other scheme in the future. To do this I've got to use the laws of physics. In some cases I discover that the reservoir knows some detail that I don't or I've overlooked, But generally speaking, they always make sense.